

2021-08

Exposure duration modulates the response of Caribbean corals to global change stressors

This work was made openly accessible by BU Faculty. Please [share](#) how this access benefits you. Your story matters.

| | |
|-------------------------------|---|
| Version | First author draft |
| Citation (published version): | H.E. Aichelman, C.B. Bove, K.D. Castillo, J.M. Boulton, A.C. Knowlton, O.C. Nieves, J.B. Ries, S.W. Davies. 2021. "Exposure duration modulates the response of Caribbean corals to global change stressors." <i>Limnology and Oceanography</i> , Volume 66, Issue 8, pp. 3100 - 3115. https://doi.org/10.1002/lno.11863 |

<https://hdl.handle.net/2144/44196>

Boston University

1 **Title:** Exposure duration modulates the response of Caribbean corals to global change stressors

2
3 **Running Title:** Exposure duration modulates coral physiology

4
5 **List of Authors:** Aichelman HE^{1,2}, Bove CB³, Castillo KD^{2,3}, Boulton JM², Knowlton AC²,
6 Nieves OC¹, Ries JB⁴, Davies SW^{1,2,4}

7
8 **Institutional Affiliations**

9 ¹Department of Biology, Boston University, Boston, MA, USA

10 ²Department of Marine Sciences, University of North Carolina at Chapel Hill, Chapel Hill, NC,
11 USA

12 ³Environment, Ecology, and Energy Program, University of North Carolina at Chapel Hill,
13 Chapel Hill, NC, USA

14 ⁴Department of Marine and Environmental Sciences, Northeastern University, Boston, MA, USA

15

16 **Contact Information:** hannahaichelman@gmail.com; (704) 607-7408

17

18 **Abstract**

19 Global change is threatening coral reefs, with rising temperatures leading to repeat bleaching
20 events (dysbiosis of coral hosts and their symbiotic algae) and ocean acidification reducing net
21 coral calcification. Although global-scale mass bleaching events are revealing fine-scale patterns
22 of coral resistance and resilience, traits that lead to persistence under environmental stress remain
23 elusive. Here, we conducted a 95-day controlled-laboratory experiment to investigate how
24 duration of exposure to ocean warming (28, 31°C), acidification ($p\text{CO}_2 = 400\text{--}2800 \mu\text{atm}$), and
25 their interaction influence the physiological responses of two Caribbean reef-building coral
26 species (*Siderastrea siderea*, *Pseudodiploria strigosa*) from two reef zones of the Belize
27 Mesoamerican Barrier Reef System. Every 30 days, calcification rate, total host protein and
28 carbohydrate, chlorophyll *a* pigment concentration, and symbiont cell density were quantified for
29 the same coral colony to characterize acclimatory responses of each genotype. Physiologies of
30 the two species were differentially affected by these stressors, with exposure duration
31 modulating responses. *Siderastrea siderea* was most affected by extreme $p\text{CO}_2$ (~2800 μatm),
32 which resulted in reduced calcification rate, symbiont density, and chlorophyll *a* concentration.
33 *Siderastrea siderea* calcification rate initially declined under extreme $p\text{CO}_2$ but recovered by the
34 final time point, and overall demonstrated resistance to next-century $p\text{CO}_2$ and temperature
35 stress. In contrast, *P. strigosa* was more negatively impacted by elevated temperature (31°C).
36 Reductions in *P. strigosa* calcification rate and total carbohydrates were consistently observed
37 over time regardless of $p\text{CO}_2$ treatment, with the greatest reductions observed under elevated
38 temperature. However, nearshore colonies of *P. strigosa* maintained calcification rates under
39 elevated temperature throughout all exposure durations, suggesting individuals from this
40 environment may be locally adapted to the warmer temperatures characterizing their natal reef
41 zone. This experiment highlights how tracking individual coral colony physiology across broad
42 exposure durations can capture acclimatory responses of corals to global change stressors.

43

44 **Keywords:** coral physiology, temperature stress, ocean acidification, *Siderastrea siderea*,
45 *Pseudodiploria strigosa*

46

47 **1. Introduction**

48 Since the Industrial Revolution, anthropogenic activities have increased the partial
49 pressure of atmospheric carbon dioxide ($p\text{CO}_2$), which has warmed the atmosphere by
50 approximately 0.6°C (Pörtner et al., 2019). As atmospheric temperatures increase, so do sea
51 surface temperatures (SSTs), a trend that has continued since 1970 (Pörtner et al., 2019).
52 Increasing atmospheric $p\text{CO}_2$ has also caused surface ocean pH to decrease at a rate of 0.017 to
53 0.027 units per decade since the 1980s, potentially exacerbating the impacts of warming SSTs on
54 marine organisms (e.g. Pörtner et al., 2019). The resulting warming and acidification have
55 impacted organisms across the globe, as thermal niches shift and habitats rapidly change (Morley
56 et al., 2018; Parmesan and Yohe, 2003; Pörtner et al., 2019). The negative effects of global
57 change are predicted to strengthen and, under the Intergovernmental Panel on Climate Change's
58 (IPCC) most extreme emissions scenario (RCP8.5), oceans are expected to take up 5 to 7 times
59 more heat and decrease by 0.3 pH units by 2100 (Pörtner et al., 2019).

60 Coral reefs are valuable economic and ecological resources (Costanza et al., 2014) that
61 are particularly vulnerable to ocean warming and acidification. The high biodiversity of coral
62 reefs depends on the obligate symbiosis between the coral animal and its symbiotic algae of the
63 family Symbiodiniaceae (previously genus *Symbiodinium*; LaJeunesse et al., 2018). This
64 symbiosis is sensitive to thermal anomalies and, because tropical coral species live within 1°C of
65 their upper thermal limit, even slight increases in SST can result in bleaching (breakdown of the
66 coral-algal symbiosis) and ultimately mortality if the symbionts fail to repopulate the coral host.
67 Global coral bleaching events are occurring with increasing frequency and severity as SST
68 continues to increase (Hughes et al., 2017).

69 Ocean acidification is the result of increased atmospheric CO_2 dissolving into seawater,
70 reducing its pH, and altering its carbonate chemistry (Doney et al., 2009; Orr et al., 2005). This

71 alteration of carbonate chemistry includes a decrease in carbonate ion concentration ($[\text{CO}_3^{2-}]$),
72 which reduces the saturation state of seawater with respect to aragonite (Ω_{arag})—which can
73 make it more challenging for corals to build their aragonite skeletons (Doney et al., 2009;
74 Kleypas et al., 1999). Laboratory experiments have shown that ocean acidification conditions
75 projected for the end of next century can have negative (Comeau et al., 2013; Hoegh-Guldberg et
76 al., 2007; Horvath et al., 2016; Kroeker et al., 2010), neutral (Reynaud et al., 2003; Ries et al.,
77 2010), and parabolic (Castillo et al., 2014) impacts on coral calcification, while field experiments
78 have yielded more negative outcomes (Albright et al., 2018; Comeau et al., 2019; Jokiel et al.,
79 2008; Kline et al., 2019). The direction and magnitude of calcification responses to acidification
80 are influenced by many factors (Kornder et al., 2018), including ability to regulate calcifying
81 fluid chemistry in support of calcification (e.g. Ries, 2011), species differences (Bove et al.,
82 2019; Okazaki et al., 2017), calcification rate under ambient conditions (Shaw et al., 2016), CO_2 -
83 induced fertilization of photosynthesis (Castillo et al., 2014), coral gender (Holcomb et al.,
84 2012), experimental duration (Kline et al., 2019), co-occurring thermal stress (Anthony et al.,
85 2011; Kroeker et al., 2013), and heterotrophic capacity (Cohen and Holcomb, 2009; Towle et al.,
86 2015). Coral calcification in response to temperature stress is similarly complicated by a number
87 of factors, and a meta-analysis by Kornder et al. (2018) highlighted strong taxonomic variation
88 and that thermal stress is more pronounced in adults and during the summer. Similar to
89 acidification, coral calcification under elevated temperature can be mediated by heterotrophic
90 capacity (Aichelman et al., 2016; Grottoli et al., 2006; Rodolfo-Metalpa et al., 2008; Towle et
91 al., 2015). In addition to considering calcification rate, energetic reserves are critical to coral
92 health and resistance to stressors, and have been associated with bleaching susceptibility

93 (Anthony et al., 2009; Grottoli et al., 2014; Levas et al., 2018) and in determining whether a
94 bleaching event will lead to mortality (Anthony et al., 2009; Grottoli et al., 2006).

95 Fewer studies consider the combined effects of temperature and acidification stress and,
96 similar to studies investigating the effects of independent stressors, such experiments have
97 produced variable results. Several studies have demonstrated that elevated temperatures have
98 stronger negative effects on the coral holobiont (combination of coral animal, algal symbiont,
99 and associated microbiota) when compared to acidification, including negative effects on
100 calcification rates (Anderson et al., 2019; Schoepf et al., 2013), larval development (Chua et al.,
101 2013), and survivorship (Anderson et al., 2019). Although no studies have found synergistic
102 effects of temperature and acidification on coral calcification (i.e. combined effects are greater
103 than sum of individual effects), numerous studies have demonstrated that the effects of
104 temperature and acidification stress can be additive, in terms of impacts on coral calcification
105 (Agostini et al., 2013; Edmunds et al., 2012; Horvath et al., 2016; Kornder et al., 2018; Prada et
106 al., 2017; Rodolfo-Metalpa et al., 2011) and metabolism (Agostini et al., 2013). A more
107 complete understanding of the combined effects of global change stressors will require
108 investigations of multiple species and stressors across longer timescales with a focus on multiple
109 physiology metrics.

110 The effects of global change on the coral holobiont not only vary by the stressors in
111 question, but also by species. Species differences in response to global change stressors have
112 been observed in coral calcification rate (Bove et al., 2019; Edmunds et al., 2012; Edmunds et
113 al., 2019; Okazaki et al., 2017) and recovery of energetic reserves through time (i.e. total soluble
114 lipid; Levas et al., 2018). Additionally, spatial scale appears to play a role in some corals'
115 responses to global change, with differential stress tolerance observed across populations along a

116 reef system (e.g. the Great Barrier Reef; Dixon et al., 2015) and across reef zones (Castillo et al.,
117 2012; Kenkel et al., 2013a; Kenkel et al., 2013b; Kenkel and Matz, 2016). Differences in coral
118 thermal tolerance can occur on spatial scales as small as between tidal pools in American Samoa
119 (Bay and Palumbi, 2014; Oliver and Palumbi, 2011; Palumbi et al., 2014), illustrating that
120 adaptation and/or acclimation to fine scale environmental differences can play a role in
121 determining coral response to global change stressors.

122 In addition to understanding stress responses across species and spatial scales,
123 considering how duration of stress exposure affects the physiological response of the coral
124 holobiont is critical (McLachlan et al., 2020). This goal is complicated by the difficulty of
125 executing long-term laboratory (*ex situ*) experiments, and it is therefore relatively rare for studies
126 to track coral physiology under controlled conditions for extended periods of time. However,
127 several studies have been conducted for approximately 90 days or more (e.g., Anderson et al.,
128 2019; Bove et al., 2019; Castillo et al., 2014; Comeau et al., 2019; Kline et al., 2019), and each
129 reveal nuanced patterns of stress and resilience in corals. For example, Comeau et al. (2019)
130 observed that acidification (1,050 $\mu\text{atm } p\text{CO}_2$) caused a rapid, but species-specific, alteration of
131 calcifying fluid chemistry in four coral and two calcifying algae species throughout the entire
132 one-year duration of the experiment (Comeau et al., 2019). Additionally, by measuring *S. siderea*
133 growth every 30 days throughout a 90-day experiment, Castillo et al. (2014) showed that
134 calcification responses to acidification (604 $\mu\text{atm } p\text{CO}_2$) varied substantially through time—with
135 calcification rates increasing in response to moderate acidification (604 $\mu\text{atm } p\text{CO}_2$) between 0
136 and 60 days, and decreasing between 60 and 90 days. Finally, Levas et al. (2018) tracked corals
137 for 11 months following experimental bleaching and found interspecific differences in the timing
138 of recovery. Specifically, *Porites divaricata* initially catabolized lipids and decreased

139 calcification but largely recovered within 11 months, while *P. astreoides* fully recovered within
140 1.5 months after increasing feeding and symbiont nitrogen uptake (Levas et al., 2018). It is
141 therefore clear that tracking coral physiology through time can provide valuable insights into
142 how corals respond to short-, moderate-, and long-term global change stress.

143 Here, two ecologically important reef-building coral species (*Siderastrea siderea* and
144 *Pseudodiploria strigosa*) from two reef zones (forereef and nearshore) of the Belize
145 Mesoamerican Barrier Reef System (MBRS) were maintained under a fully crossed acidification
146 (ca. 400 μatm [present day], ca. 640 μatm [next century], ca. 2800 μatm [extreme]) and
147 temperature (28, 31°C) experiment for 95 days. In order to characterize the responses of these
148 species to projected global change, holobiont physiology of each coral colony was monitored
149 every 30 days (exposure duration: 0-30 days = T_0 - T_{30} = short-term, 30-60 days = T_{30} - T_{60} =
150 moderate-term, 60-95 days = T_{60} - T_{95} = long-term), including metrics for both the coral host
151 (calcification rate, total protein, total carbohydrates) and symbiont (symbiont cell density,
152 chlorophyll *a* pigment concentration). The work presented here elucidates the impact of exposure
153 duration on corals' acclimatory response to global change stressors.

154

155 **2. Materials and methods**

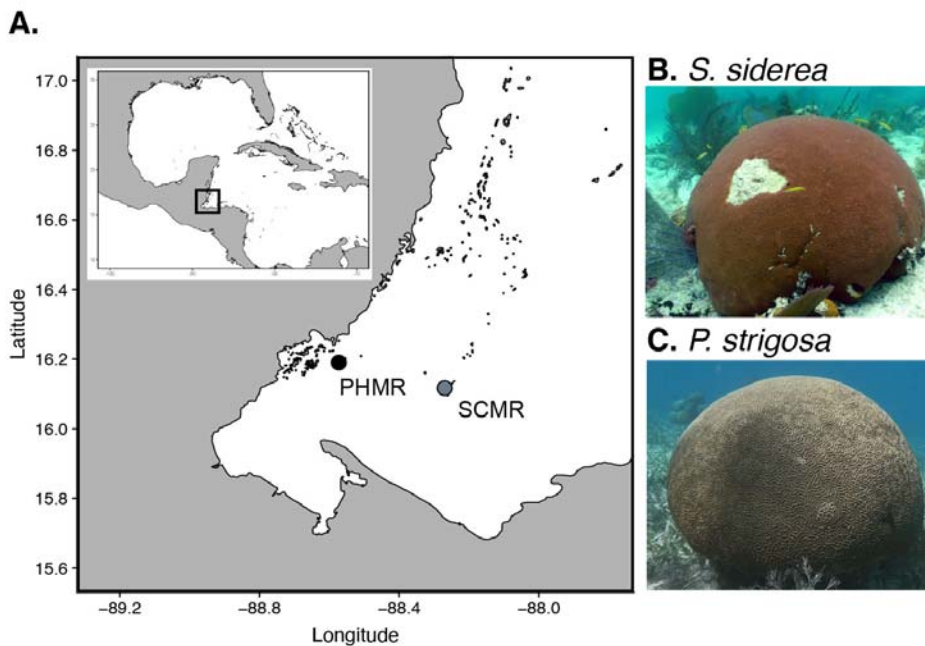
156 (2.1) Coral collection and experimental design

157 Data presented here are from an experiment run in parallel with an experiment published
158 by Bove et al. (2019). Therefore, experimental design and culturing conditions are similar to
159 those presented therein. However, data presented here pertain to a different suite of coral
160 individuals than explored in Bove et al. (2019), and only two species (instead of four) are
161 explored in the present study. Timing of the two experiments is also staggered by 30 days; for

162 comparison time T_0 in the present experiment corresponds to the “pre-acclimation period” in
163 Bove et al. (2019). Methods specific to this experiment are presented below. However, readers
164 are referred to Bove et al. (2019) for methods that pertain to both studies, such as those relating
165 to the control and monitoring of seawater carbonate chemistry parameters.

166 Three colonies of *Siderastrea siderea* and *Pseudodiploria strigosa* were collected from a
167 nearshore (NS; Port Honduras Marine Reserve, PHMR; 16°11'23.5314"N, 88°34'21.9360"W)
168 and a forereef (FR; Sapodilla Cayes Marine Reserve, SCMR; 16°07'00.0114"N,
169 88°15'41.1834"W) site along the southern portion of the Belize Mesoamerican Barrier Reef
170 System (MBRS) in June 2015 (N=3/species/site; Figure 1). Colonies were separated by at least 5
171 m to maximize the likelihood of obtaining genetically distinct individuals. Following collection,
172 all coral colonies (3 colonies x 2 reef zones x 2 species = 12 putative genotypes) were
173 transported to the Northeastern University (NU) Marine Science Center and fragmented into 24
174 genetically identical fragments. One FR *P. strigosa* colony did not survive fragmentation,
175 leaving a total of 3 genotypes for NS and FR *S. siderea*, 3 genotypes for NS *P. strigosa*, and 2
176 genotypes for FR *P. strigosa* genotypes (total of 6 *S. siderea* and 5 *P. strigosa* genotypes). After
177 fragmentation, coral fragments were allowed to recover for 23 days in natural flow-through
178 seawater with salinity and temperature (\pm SD) of 30.7 ± 0.8 and $28.2\pm 0.5^\circ\text{C}$, respectively. After
179 recovery, temperature and $p\text{CO}_2$ were incrementally adjusted over a period of 20 days until
180 target treatment conditions were achieved. During this time, temperatures of the elevated
181 temperature treatments were increased by 0.4°C every 3 days and $p\text{CO}_2$ was adjusted by $0\ \mu\text{atm}$
182 (present day), $+30\ \mu\text{atm}$ (end of century), and $+240\ \mu\text{atm}$ (extreme) every 3 days. The six
183 experimental treatments consisted of a full factorial design of two temperatures (target 28, 31°C)
184 and three $p\text{CO}_2$ levels (target 400, 700, 2800 μatm). Coral fragments were distributed such that

185 four replicate fragments from each genotype were represented in each of the six experimental
186 treatments. The six experimental treatments were replicated in three aquaria, for a total of 18 42L
187 acrylic aquaria. Each aquaria was illuminated on a 10:14 h light:dark cycle with 300 μmol
188 photons $\text{m}^{-2} \text{s}^{-1}$ of photosynthetically active radiation (PAR). The experimental system used
189 natural flow-through seawater and coral fragments were fed every other day with a mixture of
190 frozen adult *Artemia* sp. and freshly hatched *Artemia* sp.



191
192 **Figure 1.** (A) Map of coral colony collection sites from the forereef (SCMR = Sapodilla Cayes
193 Marine Reserve) and nearshore (PHMR = Port Honduras Marine Reserve) sites of the Belize
194 Mesoamerican Barrier Reef System (MBRS). (B) Example of *Siderastrea siderea* colony (photo
195 credit: K.D. Castillo). (C) Example of *Pseudodiploria strigosa* colony (photo credit: H.E.
196 Aichelman).
197

198 Coral fragments were maintained in treatment conditions for a total of 95 days (9 August
199 2015 – 12 November 2015). Average (\pm SE) $p\text{CO}_2$ and temperature conditions throughout the
200 experimental period were: 358 (\pm 131) μatm , 28.2 (\pm 0.1) $^\circ\text{C}$; 424 (\pm 40) μatm , 31.3 (\pm 0.1) $^\circ\text{C}$;
201 674 (\pm 21) μatm , 28.0 (\pm 0.1) $^\circ\text{C}$; 606 (\pm 36) μatm , 30.9 (\pm 0.1) $^\circ\text{C}$; 2750 (\pm 161) μatm , 28.4

202 (± 0.1) °C; 2917 (± 174) μatm , 31.1 (± 0.1) °C. Seawater parameters (including temperature,
203 $p\text{CO}_2$, salinity) at each time point are shown in Figure S1 and all measured and calculated
204 seawater parameters are reported in Tables S1 and S2, respectively.

205 Approximately every 30 days (exposure duration: T_0 - T_{30} days = short-term, T_{30} - T_{60} days
206 = moderate-term, T_{60} - T_{95} days = long-term), a fragment of each coral colony was removed from
207 each of the six experimental conditions, flash frozen in liquid nitrogen, and stored at -80°C for
208 subsequent analysis aimed at tracking genet-level physiology through time. In the event of
209 mortality that yielded insufficient coral fragments for sampling at all time points, corals were
210 preferentially sampled at the end of the experiment (long-term exposure: T_{95}) instead of after
211 moderate-term exposure (T_{60}). As a result, sample sizes are lower for both species at T_{60}
212 compared to the other time points. Following completion of the experiment, all remaining coral
213 fragments were flash frozen in liquid nitrogen and maintained at -80°C until subsequent
214 processing, at which time fragments were airbrushed to remove host tissue and symbiont cells.
215 Tissue slurries were homogenized using a Tissue-Tearor (Dremel; Racine, WI, USA) and
216 centrifuged to pelletize the symbiont cells. Coral host tissue and symbiont fractions were
217 separated for subsequent physiological assays.

218 (2.2) Coral host physiology measurements

219 Coral growth rates were estimated over the course of the experiment using the buoyant
220 weight technique (Davies, 1989). Buoyant weight measurements were obtained in triplicate for
221 each coral fragment at each of the four time points (T_0 , T_{30} , T_{60} , T_{95}), averaged, and normalized
222 to the coral specimens' surface area (see methods below). As in Bove et al. (2019), a subset of
223 fragments from both species were used to confirm the relationship between buoyant weight and
224 dry weight. These two measurements were correlated for both species (*S. siderea* $R^2 = 0.90$, $p <$

225 0.001; *P. strigosa* $R^2 = 0.81$, $p < 0.001$), indicating that change in buoyant weight should reflect
226 a proportionate change in dry weight. Equations used to calculate dry weight from buoyant
227 weight are shown below. Dry weight was converted from g to mg, corrected to surface area of
228 each fragment and to number of days in experimental treatment to calculate calcification rate
229 ($\text{mg cm}^{-2} \text{ day}^{-1}$).

230 *S. siderea*: Dry weight (g) = $1.95 * \text{BW (g)} + 3.60$, $R^2 = 0.90$

231 *P. strigosa*: Dry weight (g) = $1.63 * \text{BW (g)} + 6.96$, $R^2 = 0.81$

232 Growing surface area was quantified in triplicate from observed live tissue in photos of coral
233 fragments taken at each timepoint using ImageJ software (Rueden et al., 2017). The same surface
234 area values of each coral fragment were used to normalize all host and symbiont physiology
235 parameters within an experimental timepoint.

236 Because corals were frozen on the same day for each time point, there was no need to
237 correct for number of days in experimental treatment for physiological metrics other than
238 calcification rate. Total coral host protein content was quantified from host tissue slurry using a
239 bicinchoninic acid (BCA) protein assay. Host tissue slurry was vortexed with glass beads for 15
240 minutes and then centrifuged for 3 minutes at 4000 RPM. Next, 15 μL of the centrifuged sample
241 was added to 235 μL artificial seawater along with 250 μL of Bradford reagent. After samples
242 were mixed, absorbance was measured in a BioSpectrometer (Eppendorf, Hauppauge, NY, USA)
243 at 562 nm. Coral protein concentrations were calculated using a standard curve of bovine serum
244 albumin ranging from 0 to 1000 $\mu\text{g mL}^{-1}$ and normalized to living coral surface area.

245 Total host carbohydrates were quantified using the phenol-sulfuric acid method (as in
246 Masuko et al., 2005), which measures all monosaccharides, including glucose—the major
247 photosynthate translocated from symbiont to coral host (Burriesci et al., 2012). An aliquot of

248 coral host tissue was diluted to 50 μL with artificial seawater (Instant Ocean Sea Salt), to which
249 150 μL of sulfuric acid and 30 μL of 5% phenol were added. Following a 5-minute incubation at
250 90°C and another 5-minute incubation at room temperature, absorbance at 490 nm was measured
251 in a spectrophotometer (Synergy H1 Microplate Reader; BioTek Instruments; VT, USA).
252 Carbohydrate concentrations were calculated using a standard curve of D-glucose solutions
253 ranging from 0.039 to 2 mg mL^{-1} and normalized to living coral surface area.

254 (2.3) Symbiodiniaceae physiology measurements

255 Symbiont cells were quantified using the hemocytometer method similar to Rodrigues
256 and Grottoli (2007). After vortexing the symbiont pellet, a 1:1 Lugol's iodine and formalin
257 solution was added for contrast and cell preservation. Triplicate 10 μL subsamples were counted
258 on a hemocytometer using a light microscope, averaged, and normalized to slurry volume and
259 live coral tissue surface area.

260 Symbiont photosynthetic pigments (chlorophyll *a*, abbreviated Chl *a*) were quantified
261 spectrophotometrically following the method of Marchetti et al. (2012). Briefly, 40 mL of 90%
262 acetone was added to the symbiont pellet, homogenized, then stored in the dark for 24 hours. 100
263 μL of each sample was then diluted in 7.9 mL of 90% acetone. A 10AU Field and Laboratory
264 Fluorometer (Turner Designs, San Jose, CA) was used to measure the initial concentration (R_b),
265 then 2 drops of 10% HCl was added to the sample tube, after which a second fluorometer reading
266 was taken (R_a). Total Chl *a* content ($\mu\text{g L}^{-1}$) was calculated using the equation below, where
267 0.548 is a calibration constant specific to the fluorometer used, 40 mL is the volume of acetone
268 left overnight, and 80 is the dilution factor. Total Chl *a* was then normalized to live coral surface
269 area to get units of $\mu\text{g Chl } a \text{ cm}^{-2}$.

$$\text{Chl } a \left(\mu\text{g L}^{-1} \right) = 0.548 \times (R_b - R_a) \times 40\text{mL} \times 80$$

270 (2.4) Statistical analyses

271 All statistical analyses were completed using R version 3.5.2 (R Core Team, 2017). A
272 series of linear models (package *lmer*) were fitted for each species and each individual
273 physiology parameter using a forward model selection method. The best fit model was derived
274 by starting with the intercept-only model and then using forward-selection to incorporate
275 additional parameters, starting with the most significant parameter, until further addition of
276 parameters did not significantly improve the model fit. Additional parameters were retained in
277 the model if they were significant ($p < 0.05$) and produced smaller AIC values (Akaike, 1974).
278 These parameters included fixed effects of time, temperature, $p\text{CO}_2$, and reef zone, which were
279 all coded as factors. Parameter interactions were only considered if those two parameters were
280 already significant and included in the model. A random effect of genotype was included in all
281 models to account for physiological variation across genotypes. Note that for calcification rate
282 data, multiple fragments of each genotype were represented at each time point. Because
283 genotype is included in the model as a random effect, multiple fragment numbers do not
284 artificially increase the sample size and instead only increase the precision of the rate
285 measurement for that colony. The linear models used for each individual physiology parameter
286 are included along with summary statistics for *S. siderea* and *P. strigosa* in Table S3. Post-hoc
287 pairwise comparisons of significant main effects were assessed using a Tukey's HSD test,
288 implemented in the *lsmeans* function with the option "adjust = tukey". Summary statistics for all
289 post-hoc comparisons are reported in Table S4.

290 A Principal Components Analysis (PCA) was constructed using the *FactoMineR* package
291 (Lê et al., 2008) to assess how overall physiologies were modulated through time for each
292 species. All physiology parameters were log-transformed, and calcification rates were $x+2$ log-

293 transformed. Only individual coral fragments for which all physiology parameters were present
294 (calcification rate, total protein, total carbohydrate, symbiont density, Chl *a*) were included in
295 this analysis. Significance of each factor in the PCA was assessed using the *adonis()* function in
296 the *vegan* package (Oksanen, 2011), which was run with 10,000 permutations using the model
297 below. Summary statistics for all *Adonis* tests are reported in Table S5.

298
$$\text{Adonis}(\text{scores} \sim \text{reef zone} * p\text{CO}_2 * \text{temperature} + \text{genotype})$$

299 Correlation matrices of all host and symbiont physiology parameters for both species
300 through time were built using the *corrplot()* function with a significance threshold of $p = 0.05$.
301 The impacts of temperature and $p\text{CO}_2$ on all host and symbiont physiology parameters of only *P.*
302 *strigosa* were assessed via linear regression modeling, as no noteworthy correlations were found
303 for *S. siderea*. To estimate significance of the predictors and their interactions, increasingly
304 parsimonious, nested linear models (using *lmer()*) were compared with likelihood ratio tests.
305 Conditional R-squared values (accounting for both fixed and random effects) of the regressions
306 were determined using the *r.squaredGLMM()* function in the *MuMIn* package. Summary
307 statistics for all linear regressions are reported in Table S6.

308 All data and code used for the analyses presented herein can be found on the GitHub
309 repository associated with this publication

310 (https://github.com/hannahaichelman/TimeCourse_Physiology).

311

312 **3. Results**

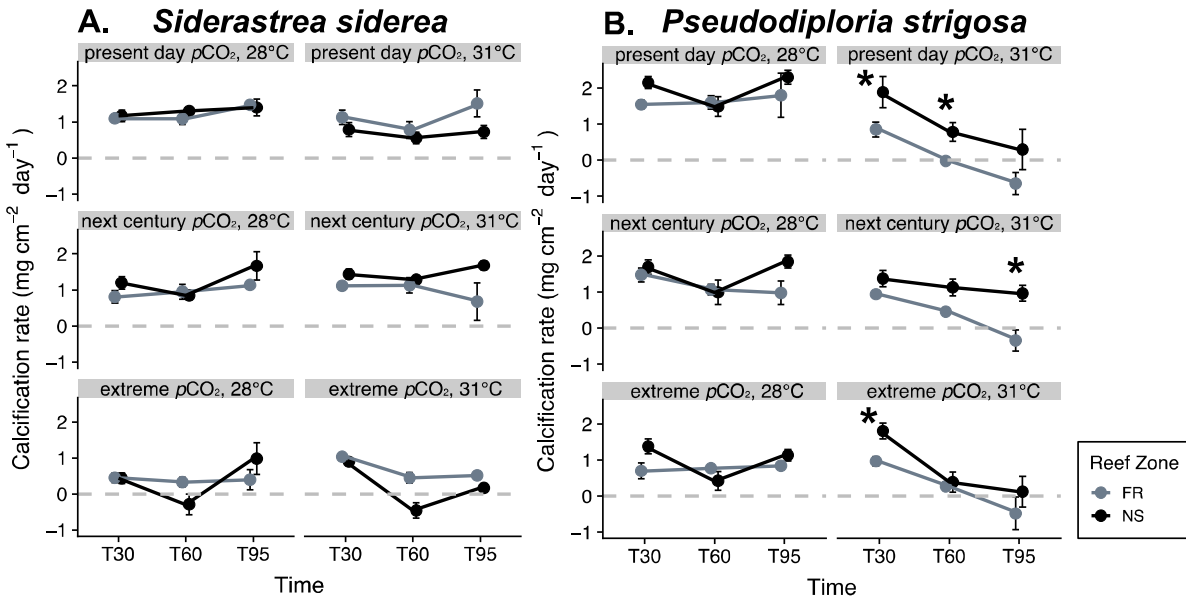
313 (3.1) Effects of thermal and acidification stress on *S. siderea* and *P. strigosa* calcification rates

314 Experiment duration ($p < 0.001$), $p\text{CO}_2$ ($p < 0.001$), and the interaction of experiment
315 duration and $p\text{CO}_2$ ($p = 0.007$), significantly influenced calcification rates of *S. siderea* (Figure

316 2A). Under extreme $p\text{CO}_2$ conditions, *S. siderea* calcification rates were significantly reduced
317 relative to both present day (Tukey $p < 0.001$) and next century (Tukey $p = 0.017$) $p\text{CO}_2$
318 treatments. Through time, calcification rates of *S. siderea* in extreme $p\text{CO}_2$ conditions declined
319 between T_{30} and T_{60} (Tukey $p < 0.001$), and also over the entire duration of the experiment (T_{30}
320 to T_{95} ; Tukey $p < 0.001$). Temperature was not included in the best-fit model, and therefore did
321 not have a significant effect on *S. siderea* calcification.

322 *P. strigosa* calcification rates were significantly affected by experiment duration ($p <$
323 0.001), $p\text{CO}_2$ ($p < 0.001$), temperature ($p < 0.001$) and reef zone ($p = 0.036$) (Figure 2B).
324 Calcification rates were reduced at elevated temperature (31°C) relative to control temperature
325 (Tukey $p < 0.001$) and nearshore corals calcified faster than forereef corals (Tukey $p = 0.039$).
326 When compared to the present day $p\text{CO}_2$ treatment, calcification rates were also reduced under
327 extreme (Tukey $p < 0.001$) and next century $p\text{CO}_2$ conditions (Tukey $p = 0.017$). A significant
328 interaction of temperature and experimental duration was also detected for *P. strigosa*
329 calcification rates ($p < 0.001$), with *P. strigosa* calcification rates decreasing between T_{30} and T_{60}
330 under both control and elevated temperatures (Tukey $p < 0.05$); however, these reductions were
331 no longer detectable after moderate- and long-term exposure (T_{60} and T_{95}). When considering the
332 full duration of the experiment (T_0 to T_{95}), *P. strigosa* calcification rates decreased under
333 elevated temperature, but not under control temperature (Figure 2B). Additionally, a significant
334 interaction between reef zone and temperature on *P. strigosa* calcification rate was detected ($p =$
335 0.031), with elevated temperatures more negatively influencing calcification of forereef corals
336 than nearshore corals (Tukey $p = 0.024$). Lastly, the interaction between temperature and $p\text{CO}_2$
337 significantly affected *P. strigosa* calcification rates ($p = 0.0009$). There were no significant
338 differences in *P. strigosa* calcification rates amongst $p\text{CO}_2$ treatments under elevated

339 temperature treatments; however, calcification rates in control temperatures were significantly
 340 reduced under extreme $p\text{CO}_2$ compared to the present day $p\text{CO}_2$ conditions (Tukey $p < 0.001$).



341
 342 **Figure 2.** *Siderastrea siderea* (A) and *Pseudodiploria strigosa* (B) calcification rate (mg cm^{-2}
 343 day^{-1}) at each experimental time point (short-term = T₃₀; moderate-term = T₆₀; long-term = T₉₅).
 344 Facets represent each of the six treatments ($p\text{CO}_2$: present day [$\sim 400 \mu\text{atm}$], next century [~ 640
 345 μatm], extreme [$\sim 2800 \mu\text{atm}$]; temperature: 28°C, 31°C) and, within a facet, data are separated
 346 by reef zone (“FR” = forereef; “NS” = nearshore). Points represent mean calcification rates since
 347 the previous time point (i.e. T₃₀ represents calcification between T₀ and T₃₀). Asterisks (*)
 348 indicate significant (Tukey $p < 0.05$) differences in calcification rates between reef zones within
 349 a time point. Error bars represent standard error. For *S. siderea* (A), each data point represents
 350 three colonies. For *P. strigosa* (B), each forereef point represents 2 colonies and each nearshore
 351 point represents 3 colonies, except at the extreme $p\text{CO}_2/28^\circ\text{C}$ treatment at T₆₀ and T₉₅, where
 352 only one forereef colony is represented due to mortality.

353
 354
 355 (3.2) Effects of thermal and acidification stress on *S. siderea* and *P. strigosa* host energy reserves

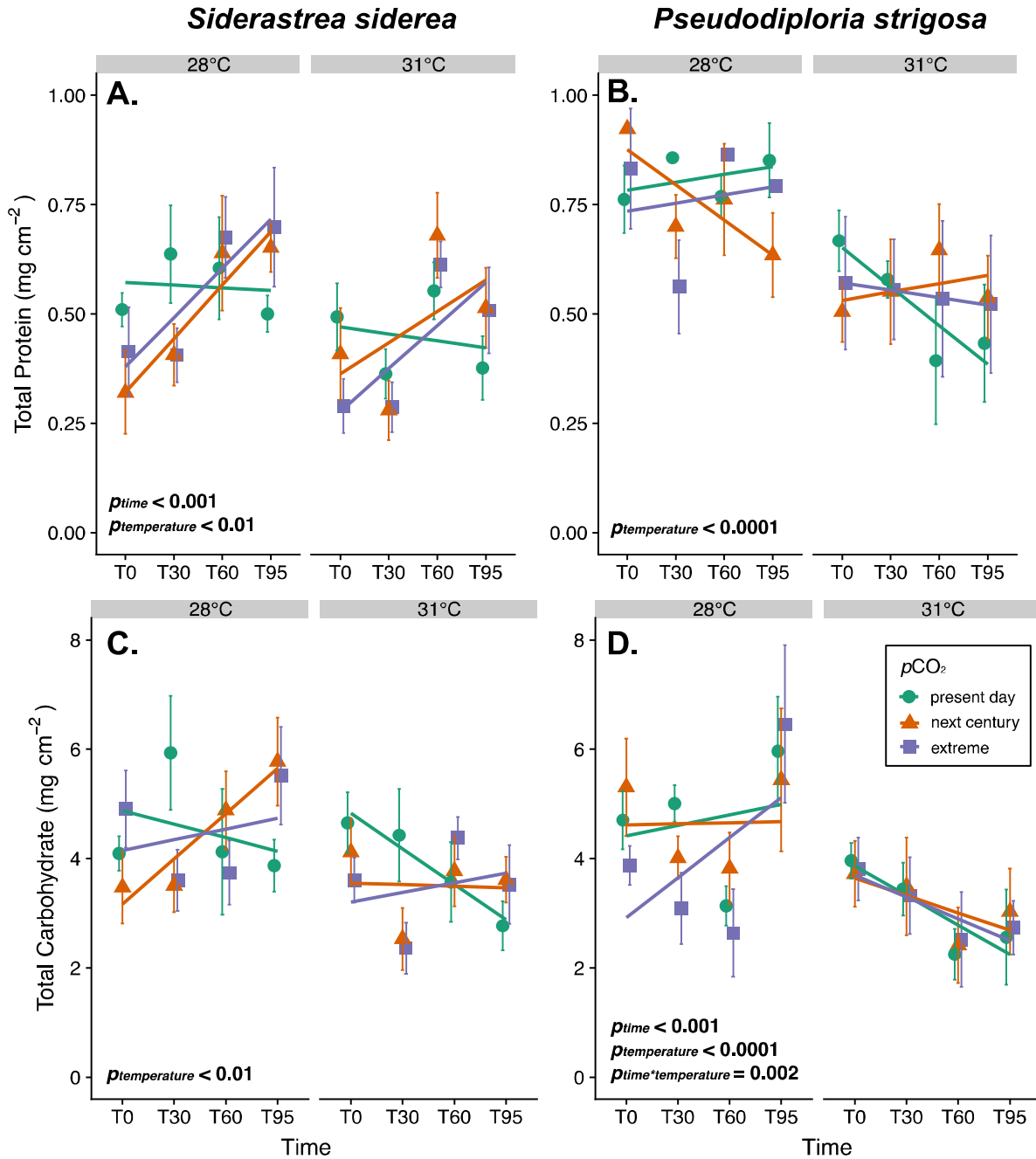
356 (3.2.1) *Siderastrea siderea* total protein and total carbohydrates

357 Both experiment duration ($p < 0.001$) and temperature ($p < 0.01$) had significant effects
 358 on *S. siderea* total protein content (Figure 3A), with elevated temperatures reducing total protein
 359 concentrations relative to corals in control temperatures (Tukey $p = 0.01$). Regardless of $p\text{CO}_2$

360 and temperature treatments, *S. siderea* total protein content increased through time, with T₉₅
361 exhibiting higher mean protein concentrations than T₀ (Tukey p = 0.03). Temperature was the
362 only factor that influenced total carbohydrates of *S. siderea* (Figure 3C; p < 0.01), with
363 significantly less carbohydrate at elevated temperature relative to the control temperature
364 treatment (Tukey p = 0.003).

365 (3.2.2) *Pseudodiploria strigosa* total protein and total carbohydrates

366 For *P. strigosa*, temperature was the only factor that significantly influenced total host
367 protein (p < 0.001), with reduced protein concentrations under elevated temperatures compared
368 to control temperature treatments (Tukey p < 0.001). However, total carbohydrate concentrations
369 were significantly affected by experiment duration (p < 0.001) and temperature (p < 0.001).
370 Similar to total protein, *P. strigosa* total carbohydrate was reduced under elevated temperatures
371 compared to control conditions (Tukey p < 0.001). Additionally, the interaction between
372 experimental duration and temperature had a significant effect on *P. strigosa* carbohydrates (p =
373 0.002), with *P. strigosa* exhibiting increasing carbohydrate concentrations between T₃₀ and T₉₅
374 under control temperatures (Tukey p = 0.004). In contrast, under elevated temperatures, *P.*
375 *strigosa* exhibited no change in carbohydrate concentrations over time (all Tukey p > 0.05),
376 although a trend of decreasing carbohydrate concentrations was observed from T₀ to T₉₅ (Figure
377 3D).



378

379 **Figure 3.** Host energy reserves (total protein [A,B] and total carbohydrate [C,D]) of *Siderastrea*
 380 *siderea* (A,C) and *Pseudodiploria strigosa* (B,D) across four experimental durations (day 0 = T₀;
 381 day 30 [short-term] = T₃₀; day 60 [moderate-term] = T₆₀; day 95 [long-term] = T₉₅). Within each
 382 panel, results are faceted by temperature treatment (28, 31°C) and colored by $p\text{CO}_2$ treatment
 383 (present day [$\sim 400 \mu\text{atm}$] = green, next century [$\sim 640 \mu\text{atm}$] = orange, extreme [$\sim 2800 \mu\text{atm}$] =
 384 purple). Each point is an average of corals from nearshore and foreereef reef zones with $n = 4-6$
 385 (*S. siderea*) and $n = 3-6$ (*P. strigosa*) distinct fragments ($n = 1$ / genotype). Significant factors are
 386 indicated in each panel. Lines represent linear fits (using ggplot2 *stat_smooth()* method to

387 visualize differences regardless of model) for each treatment through time, and error bars
388 represent standard error at each time point.

389
390 (3.3) Effects of thermal and acidification stress on symbiont physiology of *S. siderea* and *P.*

391 *strigosa*

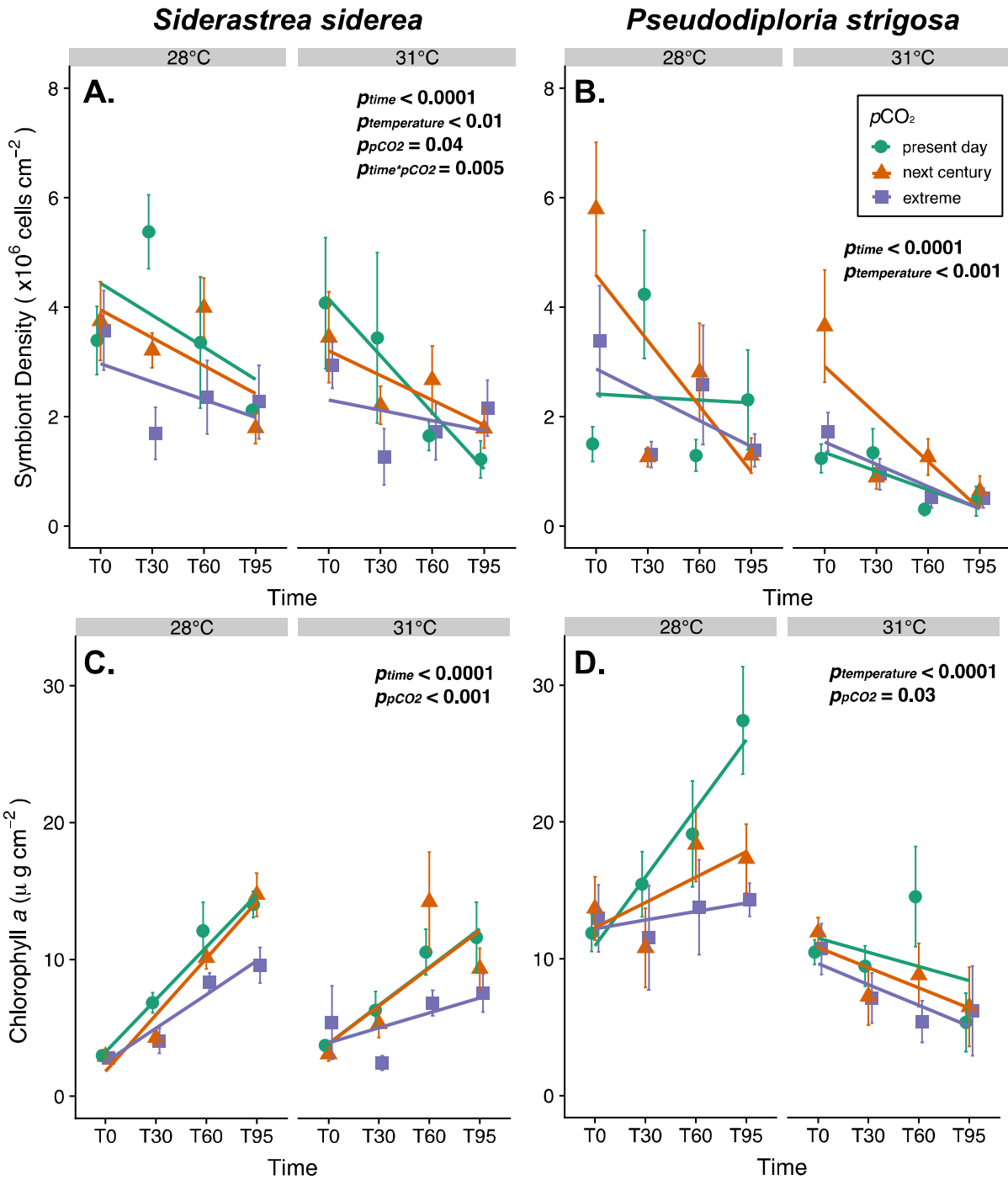
392 (3.3.1) Symbiont physiology of *S. siderea* (Chl *a* concentration, symbiont cell density)

393 Experiment duration ($p < 0.001$), temperature ($p < 0.01$), and $p\text{CO}_2$ ($p = 0.04$) had
394 significant effects on *S. siderea* symbiont cell density (Figure 4A), with cell densities decreasing
395 from T_0 to T_{95} (Tukey $p < 0.001$). Additionally, *S. siderea* cell densities were reduced under
396 elevated temperatures compared to control conditions (Tukey $p = 0.017$) and under extreme
397 $p\text{CO}_2$ compared to present day conditions (Tukey $p = 0.043$). The interaction between
398 experiment duration and $p\text{CO}_2$ also affected *S. siderea* symbiont cell density ($p = 0.005$);
399 however, within $p\text{CO}_2$ treatments the only significant change in cell densities was a decrease at
400 low $p\text{CO}_2$ between T_{30} and T_{95} (Tukey $p = 0.003$). Both experiment duration ($p < 0.001$) and
401 $p\text{CO}_2$ ($p < 0.001$) had significant effects on *S. siderea* Chl *a* concentration (Figure 4C). In
402 contrast to symbiont cell density, Chl *a* concentration increased from T_0 to T_{95} (Tukey $p <$
403 0.001). Although corals under present day and next century $p\text{CO}_2$ treatments exhibited similar
404 Chl *a* concentrations, corals under extreme $p\text{CO}_2$ had significantly less Chl *a* compared to those
405 under both present day (Tukey $p = 0.002$) and next century (Tukey $p = 0.01$) $p\text{CO}_2$ conditions.

406 (3.3.2) Symbiont physiology of *P. strigosa* (Chl *a* concentration and symbiont cell
407 density)

408 Experiment duration ($p < 0.001$) and temperature ($p < 0.001$) both had significant effects
409 on *P. strigosa* symbiont cell density. Regardless of $p\text{CO}_2$ treatment, *P. strigosa* under elevated
410 temperatures had reduced symbiont densities compared to corals in control temperatures (Tukey
411 $p < 0.001$). Additionally, *P. strigosa* symbiont density was reduced at T_{95} relative to T_0 (Tukey p

412 < 0.001). Temperature ($p < 0.001$) and $p\text{CO}_2$ treatments ($p = 0.028$) had significant effects on *P.*
413 *strigosa* Chl *a* concentration; however, experimental duration did not. Similar to symbiont
414 density, *P. strigosa* exhibited reduced Chl *a* concentrations under elevated temperatures
415 compared to control temperatures, regardless of $p\text{CO}_2$ treatment (Tukey $p < 0.001$). Additionally,
416 *P. strigosa* Chl *a* concentrations were reduced under extreme $p\text{CO}_2$ compared to present day
417 $p\text{CO}_2$ treatment regardless of temperature treatment (Tukey $p = 0.02$).
418



419

420 **Figure 4.** Symbiodiniaceae physiology (symbiont cell density [A,B] and Chl a concentration
 421 [C,D]) of *Siderastrea siderea* (A,C) and *Pseudodiploria strigosa* (B,D) across four experimental
 422 durations (day 0 = T₀; day 30 [short-term] = T₃₀; day 60 [moderate-term] = T₆₀; day 95 [long-
 423 term] = T₉₅). Within each panel, results are faceted by temperature treatment (28°C and 31°C)
 424 and colored by pCO_2 treatment (present day [~400 μ atm] = green, next century [~640 μ atm] =

425 orange, extreme [$\sim 2800 \mu\text{atm}$] = purple). Points represent averages of $n = 4-6$ (*S. siderea*) and n
426 = $3-6$ (*P. strigosa*) fragments from nearshore and forereef reef zones ($n = 1$ / genotype).
427 Significant factors are indicated in each panel. Lines represent linear fits (using ggplot2's
428 *stat_smooth()* method to visualize differences regardless of model) for each treatment through
429 time, and error bars are standard error at each time point.

430
431

432 (3.3) Holobiont physiology through time

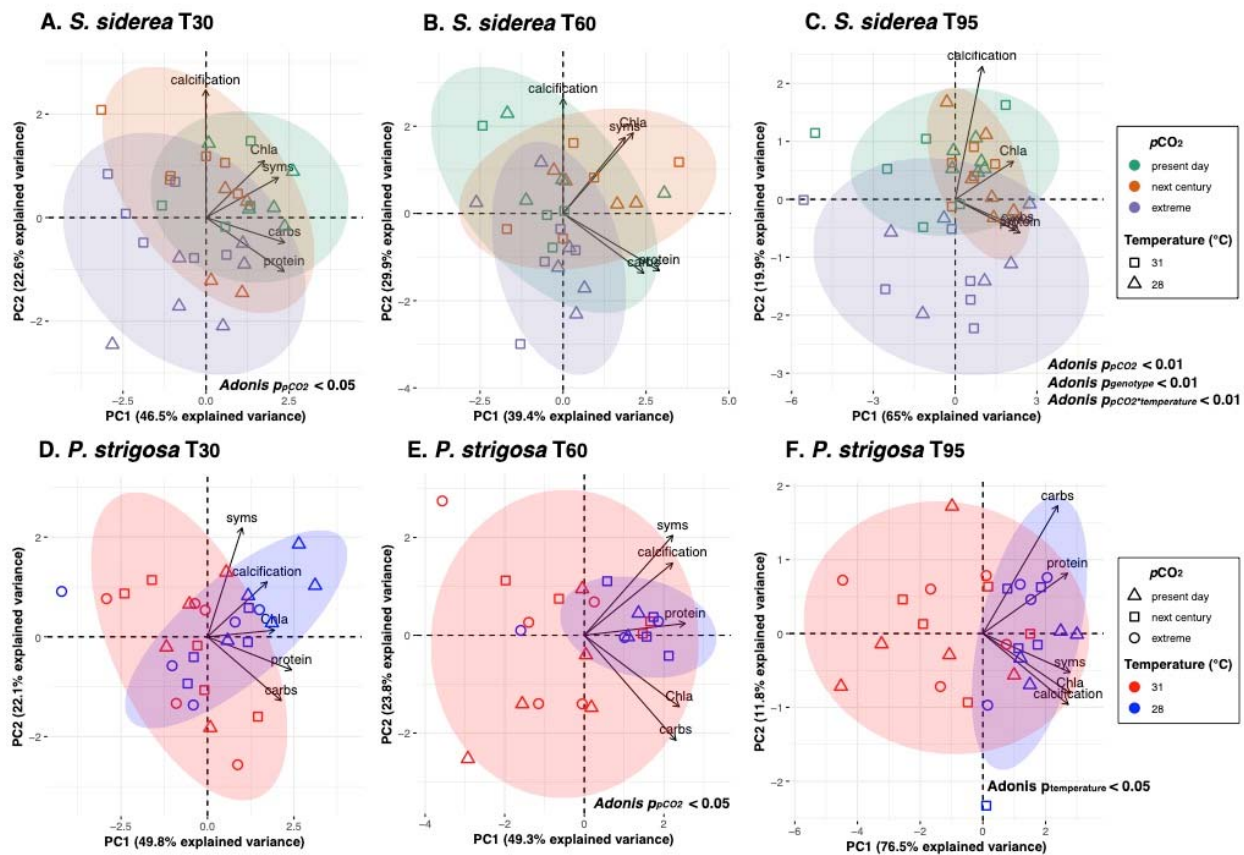
433 (3.3.1) *Siderastrea siderea* holobiont physiology

434 Overall *S. siderea* holobiont physiology clustered more strongly by $p\text{CO}_2$ than by
435 temperature (Figure 5A-C). There was a nearly significant effect of $p\text{CO}_2$ on holobiont
436 physiology after short-term exposure (T_{30} , Adonis $p = 0.054$; Figure 5A), and a significant effect
437 at T_{95} (long-term: Adonis $p = 0.002$; Figure 5C). At T_{95} , the interaction of $p\text{CO}_2$ and temperature
438 was also significant (Adonis $p = 0.001$; Figure 5C). Comparing PCAs in Figure 5A-C with
439 individual physiology results (Figures 3A,C and 4A,C) shows that $p\text{CO}_2$ significantly reduced *S.*
440 *siderea* calcification, symbiont density, and Chl *a* concentration, but did not have a significant
441 effect on total carbohydrates or protein. These results are consistent with the PCA loadings for
442 calcification, symbiont density, and Chl *a* concentration discriminating between clusters of
443 fragments in extreme $p\text{CO}_2$ treatment and the other acidification treatments (Figure 5A-C). Reef
444 zone did not have a significant main or interactive effect on *S. siderea* holobiont physiology for
445 any exposure duration.

446 (3.3.2) *Pseudodiploria strigosa* holobiont physiology

447 Holobiont physiology of *P. strigosa* clustered more strongly by temperature than by
448 $p\text{CO}_2$ treatment, especially after long-term exposure (T_{95} ; Figure 5D-F). At T_{60} (moderate-term),
449 there was a significant effect of $p\text{CO}_2$ on holobiont physiology (Adonis $p = 0.029$; Figure 5E).
450 However, at T_{95} (long-term) the effect of $p\text{CO}_2$ was no longer significant, and only temperature

451 had a significant effect (Adonis $p = 0.045$; Figure 5F). Additionally, the interaction of reef zone
 452 and temperature had a marginally significant effect on holobiont physiology after long-term
 453 exposure (T_{95} ; Adonis $p = 0.053$; Figure 5F). Comparing PCAs in Figure 5D-F with results from
 454 individual physiology parameters (Figures 3B,D and 4B,D) shows that elevated temperature had
 455 consistent negative effects on all physiology parameters.
 456



457
 458 **Figure 5. Influence of global change stressors and exposure duration on holobiont**
 459 **physiology.** Principal Components Analysis (PCA) of log-transformed holobiont physiology
 460 data, including total carbohydrate (carbs; $mg\ cm^{-2}$), total protein (protein; $mg\ cm^{-2}$), symbiont
 461 density (syms; $cells\ cm^{-2}$), chlorophyll *a* concentration (Chla; $ug\ cm^{-2}$), and calcification rate (mg
 462 $cm^{-2}\ day^{-1}$) for *Siderastrea siderea* (A-C) and *Pseudodiploria strigosa* (D-F). Colors represent
 463 pCO_2 treatment for *S. siderea* (A-C: green = present day [$\sim 400\ \mu atm$], orange = next century
 464 [$\sim 640\ \mu atm$], purple = extreme [$\sim 2800\ \mu atm$]) and temperature treatment for *P. strigosa* (D-F:
 465 red = 31°C, blue = 28°C). Shapes represent temperature treatment for *S. siderea* (A-C: square =
 466 31°C, triangle = 28°C) and pCO_2 treatment for *P. strigosa* (D-F: triangle = present day [~ 400
 467 μatm], square = next century [$\sim 640\ \mu atm$], circle = extreme [$\sim 2800\ \mu atm$]). Points represent an

468 individual coral fragment's combined physiology at each time point (**A,D** = short-term [T₃₀], **B,E**
469 = moderate-term [T₆₀], **C,F** = long-term [T₉₅]). Individuals were only included if they had data
470 for each of the five parameters at each time point. The x- and y-axes indicate the variance
471 explained (%) by the first and second principle component, respectively.
472

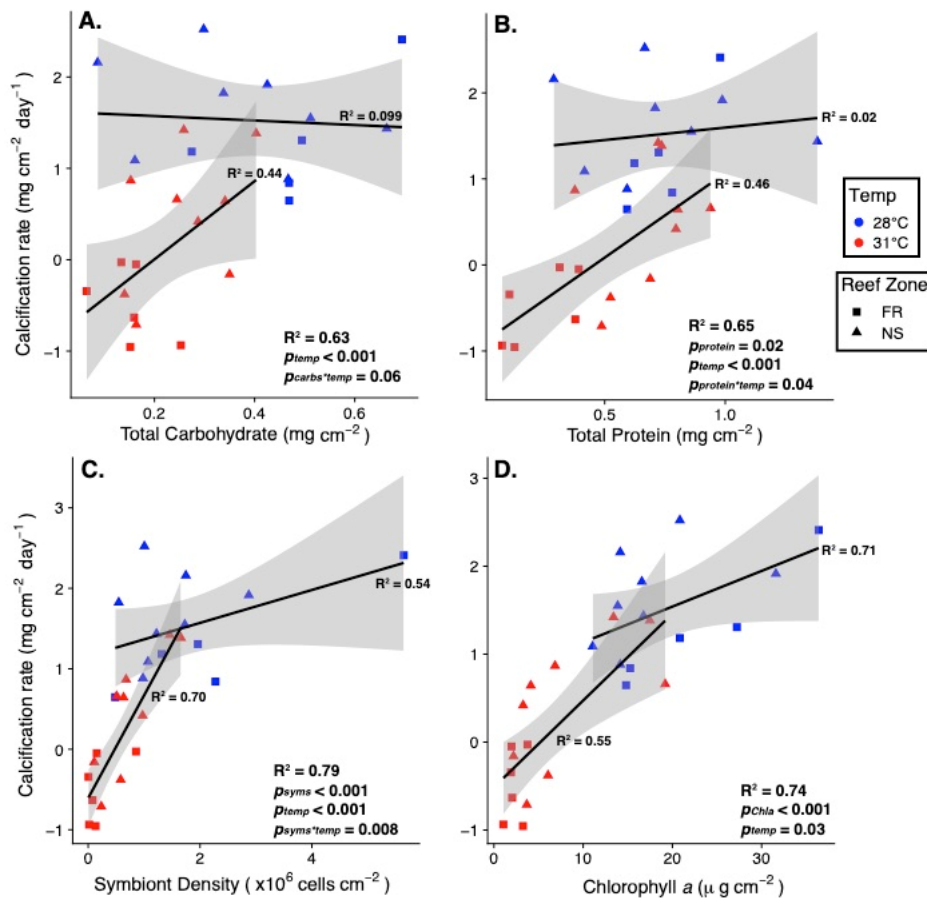
473 (3.3.3) Combined species holobiont physiology

474 *Siderastrea siderea* and *P. strigosa* had distinct holobiont physiologies at all
475 experimental durations (Adonis $p_{\text{species}} < 0.001$ for short-term [T₃₀], moderate-term [T₆₀], and
476 long-term [T₉₅]; Figure S2; Table S5). Although species had a significant main effect on
477 combined physiology through time, *S. siderea* and *P. strigosa* exhibit the most divergent
478 physiologies at T₃₀, and then converge to be entirely overlapping at T₆₀ and T₉₅ (Figure S2).
479 There were also significant independent effects of temperature and $p\text{CO}_2$ on the combined
480 physiology for both species at each time point (Adonis $p < 0.05$ for all time points; Figure S2,
481 Table S5).

482 (3.4) *Pseudodiploria strigosa* trait correlations

483 *Pseudodiploria strigosa* correlation matrices (Figure S3) revealed that calcification rate
484 was significantly correlated with all other physiology parameters ($p < 0.05$) after 95 days of
485 experimental treatment (long-term; T₉₅). As illustrated in *P. strigosa* results above, temperature
486 had a main effect on the relationship between calcification and all other predictor variables (total
487 carbohydrate and protein, symbiont density, and Chl *a* concentration; Figure 6). Correlations
488 with calcification rate were significantly different across temperature treatment for total protein
489 ($p = 0.04$) and symbiont density ($p = 0.001$) in *P. strigosa* at T₉₅ (long-term exposure). Under
490 elevated temperatures at T₉₅, *P. strigosa* fragments with higher total protein ($p = 0.04$) and
491 symbiont densities ($p = 0.001$) were able to maintain faster calcification rates (Figure 6 B,C). A
492 similar trend was observed for total carbohydrates; however, this relationship was not significant

493 (p = 0.06; Figure 6A). The interactive effect of temperature and the predictor variables on *P.*
 494 *strigosa* calcification rate was not significant until the final observation point of the experiment
 495 (T₉₅; Figure S4). *Siderastrea siderea* correlation matrix and linear regression analyses did not
 496 reveal any significant interactions with treatment.



497

498 **Figure 6.** Correlations of *Pseudodiploria strigosa* calcification rate with total host carbohydrate
 499 (A), total host protein (B), symbiont density (C), and chlorophyll *a* concentration (D) after long-
 500 term exposure to experimental treatments (T₉₅). Colors represent temperature treatment (red =
 501 31°C, blue = 28°C) and shapes represent reef zone (square = forereef [FR], triangle = nearshore
 502 [NS]). Points represent individual coral fragments. Significant factors are indicated within each
 503 panel. Lines represent linear models of measured parameters within treatment through time, fit
 504 using ggplot2's *stat_smooth()* method with gray shading representing 95% confidence intervals
 505 for each temperature. Conditional R-squared (R²) values (Nakagawa and Schielzeth, 2013) are
 506 reported for the whole model (bottom right corner of each facet) and for each temperature (next
 507 to the line of best fit).
 508

509

510

511 **4. Discussion**

512 (4.1) *Siderastrea siderea* and *P. strigosa* exhibit divergent responses to warming and
513 acidification

514 Our results demonstrate that *S. siderea* and *P. strigosa* exhibit divergent responses to two
515 co-occurring global change stressors—warming and acidification— and that these responses are
516 modulated by exposure duration (i.e. short-term = T_0 - T_{30} , moderate-term = T_{30} - T_{60} , and long-
517 term = T_{60} - T_{95}). Overall physiological performance of *S. siderea* was more negatively affected
518 by acidification through time (Figure 5A-C), while temperature stress had a more negative effect
519 on *P. strigosa* physiology through time (Figure 5D-F). Such species-specific responses to
520 temperature and acidification are not uncommon in reef-building corals. For example, when
521 testing how twelve Caribbean coral species responded to crossed temperature and acidification
522 conditions for six weeks, Okazaki et al. (2017) observed some species exhibited no growth
523 response to either temperature or acidification (including *S. siderea* and *P. strigosa*), while other,
524 more abundant Florida species (e.g. *O. faveolata* and *P. astreoides*) exhibited decreased
525 calcification rates under both stressors. In contrast to Okazaki et al. (2017), we find that *S.*
526 *siderea* and *P. strigosa* holobiont physiology was significantly affected by acidification and
527 elevated temperature, respectively. Although this difference may be due to the duration of
528 experimental stress (>30 days longer than Okazaki et al. (2017)), it could also be a result of
529 Okazaki et al. (2017) using less extreme treatments (30.3°C and 1300 μ atm $p\text{CO}_2$) than those
530 used here (31°C and 2800 μ atm). It is also possible that populations of *S. siderea* and *P. strigosa*
531 in the Florida Keys, the source of corals used in the Okazaki et al. (2017) study, could be less

532 susceptible to stress than populations from the southern MBRS used here. According to the
533 climate variability hypothesis (CVH; Stevens, 1989), higher latitude populations (e.g. Florida
534 Keys) that experience more variable thermal regimes are predicted to be more phenotypically
535 flexible and exhibit a wider range of thermal tolerances compared to populations existing closer
536 to the equator (e.g. MBRS; Bozinovic et al., 2011). In a meta-analysis of Caribbean coral
537 calcification responses to acidification, elevated temperature, and the combination of the two
538 stressors, Bove et al. (2020) found similar regional differences in stress responses between corals
539 from the Florida Keys and Belize. While calcification of Florida Keys corals did not clearly
540 respond to acidification, elevated temperature, or their combination, elevated temperature
541 reduced calcification rates in corals from Belize (Bove et al., 2020). While acknowledging
542 differences in annual temperature variability, Bove et al. (2020) highlight differences in
543 experimental treatment extremes as the main driver of calcification. While consideration of
544 treatment level is critical, such population-level differences in stress tolerance have been
545 previously observed in corals, for example in *Acropora millepora* across 5° of latitude on the
546 Great Barrier Reef (Dixon et al., 2015). Regardless, results of the present study contribute to a
547 growing body of literature supporting *S. siderea*'s resistance to conditions of elevated
548 temperature and acidification (Banks and Foster, 2016; Bove et al., 2019; Castillo et al., 2014;
549 Castillo et al., 2011; Davies et al., 2016).

550 High resistance of *S. siderea* to global change stressors was previously reported by
551 Castillo et al. (2014), which found that only the most extreme temperature (32°C) and
552 acidification (2553 $\mu\text{atm } p\text{CO}_2$) treatments resulted in reduced calcification rates. In the context
553 of global change scenarios projected by the IPCC, Castillo et al. (2014) concluded that *S. siderea*
554 will be more negatively impacted by elevated temperatures over the coming century, given that

555 the IPCC's next-century acidification projections did not reduce calcification rates. The findings
556 of the present study are consistent with this previous work, as only the extreme $p\text{CO}_2$ treatment–
557 but not next century $p\text{CO}_2$ treatment–reduced calcification rate in *S. siderea* (Figure 2A). Gene
558 expression profiling of *S. siderea* from the Castillo et al. (2014) coral fragments revealed that
559 thermal stress caused large-scale down regulation of gene expression, while acidification stress
560 elicited upregulation of proton transport genes (Davies et al., 2016), potentially offsetting the
561 effects of acidification at the site of calcification (e.g. Ries, 2011; Schoepf et al., 2017). These
562 findings provide further support for *S. siderea*'s ability to acclimate to acidification stress.

563 Bove et al. (2019) investigated the combined effects of similar temperature and
564 acidification treatments on four species of reef building corals: *S. siderea*, *P. strigosa*, *Porites*
565 *astreoides*, and *Undaria tenuifolia*. After 93 days, all species exhibited calcification declines
566 under increased $p\text{CO}_2$. However, *P. strigosa* was the only species that exhibited reduced
567 calcification under elevated temperature, which is consistent with results present here and
568 highlights that thermal stress more negatively impacts *P. strigosa* than *S. siderea* (Figure 5D-F).
569 Bove et al. (2019) also found that *S. siderea* was the most resistant of the four species studied, as
570 it was able to maintain positive calcification rates even in the most extreme acidification
571 treatment ($\sim 3300 \mu\text{atm } p\text{CO}_2$)—findings that are also corroborated here (Figure 2A).
572 Interestingly, by quantifying net calcification rates at 30-day increments, we show that *S. siderea*
573 net calcification was negative under extreme $p\text{CO}_2$ at T_{60} and then these rates recovered by T_{95}
574 (Figure 2A). This suggests that these corals are acclimating to stressful conditions over time,
575 perhaps through transcriptome plasticity, as previously proposed by Davies et al. (2016).

576 (4.2) Stress differentially modulates coral physiology across species

577 Under thermal and acidification stress, corals can draw on energy reserves, including
578 lipids, proteins, and carbohydrates, to maintain and/or produce tissue and skeleton (Anthony et
579 al., 2009; Schoepf et al., 2013). In addition to using energetic reserves, heterotrophic feeding
580 (Aichelman et al., 2016; Drenkard et al., 2013; Edmunds, 2011; Towle et al., 2015) or enhanced
581 productivity of Symbiodiniaceae owing to CO₂ fertilization of symbiont photosynthesis (Brading
582 et al., 2011) can augment energetic resources in zooxanthellate corals. Coral energetic reserves
583 can therefore influence resistance to and recovery from stress events (Edmunds et al., 2016;
584 Grottoli et al., 2006; Grottoli et al., 2014; Schoepf et al., 2015).

585 Results of the present study show that the host energy reserves (protein, carbohydrates) of
586 *S. siderea* and *P. strigosa* responded to global change stress (warming, acidification) in different
587 ways. Between T₀ and T₆₀, *P. strigosa* exhibited reduced carbohydrates regardless of treatment,
588 indicating catabolism of this energy reserve (Figure 3D). This was followed by the restoration of
589 carbohydrates (i.e. acclimation) at control temperatures at T₉₅ (Figure 3D), which likely
590 supported the positive calcification rates also observed under these conditions (Figure 6A, Figure
591 S4). Protein reserves do not show the same trend as carbohydrates through time (Figure 3B),
592 potentially owing to *P. strigosa* catabolizing carbohydrates before proteins, which has been
593 observed over shorter time scales for other scleractinian coral species (Grottoli et al., 2004).
594 However, elevated protein reserves did predict faster calcification rates in *P. strigosa* under
595 elevated temperatures, but not until the final observation point of the experiment (T₉₅; Figure 6B,
596 Figure S4). As photosynthate translocated from symbionts is a major source of carbohydrates to
597 the coral host (Burriesci et al., 2012; Muscatine, 1990), reductions in symbiont cell density, Chl
598 *a* concentration, and carbohydrates of *P. strigosa* at elevated temperature suggest that symbionts
599 were translocating fewer resources to the host, which likely contributed to observed reductions in

600 calcification under these elevated temperature conditions, particularly after long-term exposure
601 (T_{95} , Figure 6). Total protein and carbohydrate abundances of *S. siderea*, similar to those of *P.*
602 *strigosa*, declined under elevated temperatures (Figure 3A,C)—consistent with previous work
603 highlighting upregulation of protein catabolism pathways in *S. siderea* exposed to long-term
604 thermal stress (Davies et al., 2016).

605 An overall trend in reduced symbiont density and increased Chl *a* concentration through
606 time were observed under most pCO_2 and temperature conditions, except for *P. strigosa* under
607 elevated temperature (Figure 4). Given that both species under most treatments exhibited this
608 pattern, it cannot be ruled out that these changes in symbiont physiology were influenced by
609 other factors, including incomplete symbiont acclimation to experimental light environment
610 (Roth, 2014) and seasonal patterns in symbiont density and pigment concentration (Fitt et al.,
611 2000)—which may have masked the symbiont response to thermal stress within *S. siderea*. In
612 contrast, *P. strigosa* exhibited reduced symbiont density and Chl *a* concentrations under elevated
613 temperature (Figure 4B,D), a pattern that is more consistent with thermally induced bleaching
614 (Brown, 1997; Fitt et al., 2001; Glynn, 1993; Warner et al., 1999; Weis, 2008) and further
615 illustrates the susceptibility of this species to thermal stress.

616 (4.3) Nearshore *P. strigosa* are more resistant than forereef conspecifics

617 Natal reef zone was a significant predictor of host physiology, particularly for *P. strigosa*,
618 as nearshore corals calcified faster overall (Figure 2B). Although reef zone differences in
619 calcification were observed for *S. siderea* (particularly through time), colonies from one reef
620 zone did not clearly outperform colonies from the other reef zone (Figure 2A). In contrast, the
621 reef-zone-specific calcification response of *P. strigosa* may arise from local adaptation of the
622 host to distinct temperature regimes. On the MBRS, nearshore habitats are characterized by

623 higher maximum temperatures, greater annual temperature range, and more days above the
624 regional thermal bleaching threshold compared to forereef sites (Baumann et al., 2016). Local
625 adaptation to distinct reef zones is not uncommon in corals, and has been previously shown to
626 affect responses of corals to thermal stress. For example, *P. astreoides* was previously found to
627 be locally adapted to distinct thermal regimes in the Florida Keys, with inshore corals
628 demonstrating higher thermal tolerance, constitutively higher expression of specific metabolic
629 genes, and greater gene expression plasticity compared to offshore conspecifics (Kenkel et al.,
630 2013a; Kenkel et al., 2013b; Kenkel and Matz, 2016). Additionally, *P. strigosa* is a
631 hermaphroditic broadcast spawning species, and previous work on populations from the Flower
632 Garden Banks demonstrated that larvae have short pelagic larval durations (PLD; Davies et al.,
633 2017), which could facilitate local adaptation as larvae are more likely to locally recruit (Davies
634 et al., 2017; Mayorga-Adame et al., 2017). However, it is unknown if *P. strigosa* on the MBRS
635 have similarly short PLDs. We hypothesize that nearshore *P. strigosa* are locally adapted and/or
636 acclimated to more variable and stressful nearshore conditions, allowing maintenance of higher
637 calcification rates under thermal stress compared to their forereef counterparts.

638 It is important to note that responses to stress based on reef zone could be obscured by
639 uneven sampling across reef zones, as forereef genotypes of *P. strigosa* were slightly
640 underrepresented in the experiment (2 genotypes present vs. the standard 3) due to mortality
641 before the experiment began. It is possible that full replication of genotype would have yielded
642 different effects of reef zone in other *P. strigosa* physiology parameters.

643 Although the *S. siderea* PLD is unknown, previous work has shown high population
644 connectivity across 2,000 km of the Brazil coast (Nunes et al., 2011). If MBRS *S. siderea*
645 populations are similarly connected, it is possible that no genetic differences exist across

646 nearshore and forereef environments—potentially explaining the lack of reef-zone-specific
647 responses observed here. Yet this result is inconsistent with previous findings that forereef
648 colonies of MBRS *S. siderea* exhibited greater physiological stress than inshore colonies when
649 exposed to higher temperatures (Castillo and Helmuth, 2005), reduced skeletal extension rates
650 relative to inshore colonies over multi-decadal warming of the reef system (Castillo et al., 2012),
651 and reduced symbiont photophysiology relative to inshore colonies under higher temperatures
652 (Davies et al., 2018). However, consistent with results presented here, Bove et al. (2019) also
653 found no evidence for reef-zone differences in physiology for *S. siderea*, or for any of the other
654 species tested. Nevertheless, the observation that both nearshore and forereef *S. siderea*
655 performed well under global change stressors provides further support for resistance of this
656 species.

657 (4.4) Time-course experiments reveal acclimation to thermal stress in two common Caribbean
658 corals

659 This study contributes to a growing body of literature demonstrating the value of
660 assessing time-course physiology of corals exposed to global change stressors. Although studies
661 investigating independent effects of temperature and acidification on scleractinian corals have
662 yielded great insight into the effects of future global change on coral systems (e.g. Albright et al.,
663 2018; Anthony et al., 2011; Carricart-Ganivet et al., 2012; Comeau et al., 2013; Jokiel and Coles,
664 1990; Jury et al., 2010), the combined effects of these stressors remain less explored—
665 particularly in the context of how the coral stress response is modulated by the duration of those
666 stressors. By characterizing coral host and symbiont physiology of a colony through time,
667 acclimatory responses were identified in two common Caribbean reef-building coral species. The
668 results of this study provide further evidence of the species-specific nature of this acclimation.

669 For example, under extreme $p\text{CO}_2$ and elevated temperature, *S. siderea* calcification rate appears
670 to recover by the end of the experiment while *P. strigosa* calcification rate declines into negative
671 net calcification. In addition to furthering our understanding of how corals could respond to
672 projected future ocean conditions, the exposure duration component of this study suggests that
673 species will exhibit differential persistence through ephemeral stress events. It is clear that local
674 heat waves that raise SST and upwelling events that reduce pH, which already threaten coral
675 populations, may threaten coral species in different ways in the future depending on the
676 timescales of these events.

677 Acclimation is an important mechanism by which corals can withstand changing
678 environmental conditions, and transcriptome plasticity is one way by which corals can acclimate
679 to stress (Davies et al., 2016; Kenkel and Matz, 2016). A coral reciprocal transplant study
680 between reef zones in the Florida Keys demonstrated that adaptive gene expression plasticity,
681 specifically plasticity of stress response genes, was associated with reduced susceptibility to a
682 summer bleaching event (Kenkel and Matz, 2016). In addition to plasticity providing a
683 mechanism for acclimation within a generation, rapid evolutionary adaptation of corals to
684 warmer oceans has also been observed on the Great Barrier Reef (Dixon et al., 2015; Matz et al.,
685 2018). However, recent widespread declines in coral abundance, diversity, and health suggest
686 that rates of intra- and trans-generational adaptation to global change stressors within most coral
687 populations are insufficient for mitigating the deleterious impacts of recent and future CO_2 -
688 induced global change (Thomas et al., 2018). Understanding the interplay of acclimation and
689 adaptation in scleractinian corals is therefore essential for projecting how coral reef ecosystems
690 will fare in the higher- CO_2 future (Chevin et al., 2010; Thomas et al., 2018). This study furthers
691 understanding of how exposure duration modulates coral physiology across reef zones in two

692 prevalent Caribbean reef-building species. Future studies focusing on long-term acclimation
693 capacities of corals will further elucidate mechanisms of resistance and resilience in corals'
694 response to global stressors.

695

696

697

698

699 **5. Acknowledgements**

700 We thank the Belize Fisheries Department for all coral collection permits. Isaac Westfield,
701 Amanda Dwyer, Sara Williams, and Louise Cameron are acknowledged for assisting with
702 experimental maintenance at Northeastern University. Thanks to both the Marchetti and Septer
703 labs at the University of North Carolina at Chapel Hill (UNC) for assistance with equipment and
704 lab space to complete the physiology assays. We also thank Samir Patel, Savannah Swinea,
705 Bailey Thomasson, Forrest Buckthal, and Cori Lopazanski for assisting with preparing corals for
706 physiology assays at UNC.

707

708 **6. Funding**

709 This project was supported by NSF award OCE-1437371 (to J.B.R.), NSF award OCE-1459522
710 (to K.D.C.), NOAA award NA13OAR4310186 (to J.B.R. and K.D.C.), and the National
711 Academies of Sciences, Engineering, and Medicine Gulf Research Program Fellowship (to
712 S.W.D.). H.E.A. was supported by an NSF GRFP (2016222953) and S.W.D. was a Simons
713 Foundation Fellow of the Life Sciences Research Foundation (LSRF) while completing part of
714 this research.

715

716 **7. References**

- 717 **Agostini, S., Fujimura, H., Higuchi, T., Yuyama, I., Casareto, B. E., Suzuki, Y. and**
718 **Nakano, Y.** (2013). The effects of thermal and high-CO₂ stresses on the metabolism and
719 surrounding microenvironment of the coral *Galaxea fascicularis*. *Comptes rendus*
720 *biologies* **336**, 384-391.
- 721 **Aichelman, H. E., Townsend, J. E., Courtney, T. A., Baumann, J. H., Davies, S. W. and**
722 **Castillo, K. D.** (2016). Heterotrophy mitigates the response of the temperate coral
723 *Oculina arbuscula* to temperature stress. *Ecol. Evol* **6**, 6758-6769.
- 724 **Akaike, H.** (1974). A new look at the statistical model identification. *IEEE transactions on*
725 *automatic control* **19**, 716-723.
- 726 **Albright, R., Takeshita, Y., Koweek, D. A., Ninokawa, A., Wolfe, K., Rivlin, T., Nebuchina,**
727 **Y., Young, J. and Caldeira, K.** (2018). Carbon dioxide addition to coral reef waters
728 suppresses net community calcification. *Nature* **555**, 516.
- 729 **Anderson, K. D., Cantin, N. E., Casey, J. M. and Pratchett, M. S.** (2019). Independent effects
730 of ocean warming versus acidification on the growth, survivorship and physiology of two
731 *Acropora* corals. *Coral Reefs* **38**, 1225-1240.
- 732 **Anthony, K. R., Hoogenboom, M. O., Maynard, J. A., Grottoli, A. G. and Middlebrook, R.**
733 (2009). Energetics approach to predicting mortality risk from environmental stress: a case
734 study of coral bleaching. *Funct Ecol* **23**, 539-550.
- 735 **Anthony, K. R., Maynard, J. A., DIAZ-PULIDO, G., Mumby, P. J., Marshall, P. A., Cao,**
736 **L. and HOEGH-GULDBERG, O.** (2011). Ocean acidification and warming will lower
737 coral reef resilience. *Global Change Biology* **17**, 1798-1808.
- 738 **Banks, S. and Foster, K.** (2016). Baseline levels of *Siderastrea siderea* bleaching under normal
739 environmental conditions in Little Cayman. *Open Journal of Marine Science* **7**, 142-154.
- 740 **Baumann, J. H., Townsend, J. E., Courtney, T. A., Aichelman, H. E., Davies, S. W., Lima,**
741 **F. P. and Castillo, K. D.** (2016). Temperature regimes impact coral assemblages along
742 environmental gradients on lagoonal reefs in Belize. *PloS one* **11**, e0162098.
- 743 **Bay, R. A. and Palumbi, S. R.** (2014). Multilocus adaptation associated with heat resistance in
744 reef-building corals. *Curr Biol* **24**, 2952-2956.
- 745 **Bove, C., Umbanhowar, J. and Castillo, K. D.** (2020). Meta-analysis reveals reduced coral
746 calcification under projected ocean warming but not under acidification across the
747 Caribbean Sea. *Frontiers in Marine Science* **7**, 127.
- 748 **Bove, C. B., Ries, J. B., Davies, S. W., Westfield, I. T., Umbanhowar, J. and Castillo, K. D.**
749 (2019). Common Caribbean corals exhibit highly variable responses to future
750 acidification and warming. *Proceedings of the Royal Society B* **286**, 20182840.
- 751 **Bozinovic, F., Calosi, P. and Spicer, J. I.** (2011). Physiological correlates of geographic range
752 in animals. *Annu. Rev. Ecol. Evol. Syst.* **42**, 155-179.
- 753 **Brading, P., Warner, M. E., Davey, P., Smith, D. J., Achterberg, E. P. and Suggett, D. J.**
754 (2011). Differential effects of ocean acidification on growth and photosynthesis among
755 phylotypes of *Symbiodinium* (Dinophyceae). *Limnol Oceanogr* **56**, 927-938.
- 756 **Brown, B. E.** (1997). Coral bleaching: causes and consequences. *Coral reefs* **16**, S129-S138.
- 757 **Burriesci, M. S., Raab, T. K. and Pringle, J. R.** (2012). Evidence that glucose is the major
758 transferred metabolite in dinoflagellate–cnidarian symbiosis. *J. Exp. Biol.* **215**, 3467-
759 3477.

- 760 **Carricart-Ganivet, J. P., Cabanillas-Teran, N., Cruz-Ortega, I. and Blanchon, P.** (2012).
761 Sensitivity of calcification to thermal stress varies among genera of massive reef-building
762 corals. *PLoS One* **7**, e32859.
- 763 **Castillo, K. and Helmuth, B.** (2005). Influence of thermal history on the response of
764 *Montastraea annularis* to short-term temperature exposure. *Mar. Biol* **148**, 261-270.
- 765 **Castillo, K. D., Ries, J. B., Bruno, J. F. and Westfield, I. T.** (2014). The reef-building coral
766 *Siderastrea siderea* exhibits parabolic responses to ocean acidification and warming.
767 *Proceedings of the Royal Society of London B: Biological Sciences* **281**, 20141856.
- 768 **Castillo, K. D., Ries, J. B. and Weiss, J. M.** (2011). Declining coral skeletal extension for
769 forereef colonies of *Siderastrea siderea* on the Mesoamerican Barrier Reef System,
770 Southern Belize. *PLoS One* **6**.
- 771 **Castillo, K. D., Ries, J. B., Weiss, J. M. and Lima, F. P.** (2012). Decline of forereef corals in
772 response to recent warming linked to history of thermal exposure. *Nat. Clim. Change*. **2**,
773 756.
- 774 **Chevin, L.-M., Lande, R. and Mace, G. M.** (2010). Adaptation, plasticity, and extinction in a
775 changing environment: towards a predictive theory. *PLoS biology* **8**, e1000357.
- 776 **Chua, C. M., Leggat, W., Moya, A. and Baird, A. H.** (2013). Temperature affects the early life
777 history stages of corals more than near future ocean acidification. *Mar Ecol Prog Ser*.
778 **475**, 85-92.
- 779 **Cohen, A. L. and Holcomb, M.** (2009). Why corals care about ocean acidification: uncovering
780 the mechanism. *Oceanography* **22**, 118-127.
- 781 **Comeau, S., Carpenter, R. and Edmunds, P.** (2013). Coral reef calcifiers buffer their response
782 to ocean acidification using both bicarbonate and carbonate. *Proceedings of the Royal*
783 *Society B: Biological Sciences* **280**, 20122374.
- 784 **Comeau, S., Cornwall, C., DeCarlo, T., Doo, S., Carpenter, R. and McCulloch, M.** (2019).
785 Resistance to ocean acidification in coral reef taxa is not gained by acclimatization. *Nat.*
786 *Clim. Change*. **9**, 477.
- 787 **Costanza, R., de Groot, R., Sutton, P., Van der Ploeg, S., Anderson, S. J., Kubiszewski, I.,**
788 **Farber, S. and Turner, R. K.** (2014). Changes in the global value of ecosystem
789 services. *Global environmental change* **26**, 152-158.
- 790 **Davies, P. S.** (1989). Short-term growth measurements of corals using an accurate buoyant
791 weighing technique. *Mar. Biol* **101**, 389-395.
- 792 **Davies, S. W., Marchetti, A., Ries, J. B. and Castillo, K. D.** (2016). Thermal and pCO₂ stress
793 elicit divergent transcriptomic responses in a resilient coral. *Frontiers in Marine Science*
794 **3**, 112.
- 795 **Davies, S. W., Ries, J. B., Marchetti, A. and Castillo, K. D.** (2018). Symbiodinium functional
796 diversity in the coral *Siderastrea siderea* is influenced by thermal stress and reef
797 environment, but not ocean acidification. *Frontiers in Marine Science* **5**, 150.
- 798 **Davies, S. W., Strader, M. E., Kool, J. T., Kenkel, C. D. and Matz, M. V.** (2017). Modeled
799 differences of coral life-history traits influence the refugium potential of a remote
800 Caribbean reef. *Coral Reefs* **36**, 913-925.
- 801 **Dixon, G. B., Davies, S. W., Aglyamova, G. V., Meyer, E., Bay, L. K. and Matz, M. V.**
802 (2015). Genomic determinants of coral heat tolerance across latitudes. *Science* **348**, 1460-
803 1462.
- 804 **Doney, S. C., Fabry, V. J., Feely, R. A. and Kleypas, J. A.** (2009). Ocean acidification: the
805 other CO₂ problem. *Ann Rev Mar Sci.* **1**, 169-192.

- 806 **Drenkard, E. J., Cohen, A. L., McCorkle, D. C., de Putron, S. J., Starczak, V. R. and Zicht,**
807 **A.** (2013). Calcification by juvenile corals under heterotrophy and elevated CO₂. *Coral*
808 *Reefs* **32**, 727-735.
- 809 **Edmunds, P. J.** (2011). Zooplanktivory ameliorates the effects of ocean acidification on the reef
810 coral *Porites* spp. *Limnol Oceanogr* **56**, 2402-2410.
- 811 **Edmunds, P. J., Brown, D. and Moriarty, V.** (2012). Interactive effects of ocean acidification
812 and temperature on two scleractinian corals from Moorea, French Polynesia. *Global*
813 *Change Biology* **18**, 2173-2183.
- 814 **Edmunds, P. J., Comeau, S., Lantz, C., Andersson, A., Briggs, C., Cohen, A., Gattuso, J.-P.,**
815 **Grady, J. M., Gross, K. and Johnson, M.** (2016). Integrating the effects of ocean
816 acidification across functional scales on tropical coral reefs. *Bioscience* **66**, 350-362.
- 817 **Edmunds, P. J., Doo, S. S. and Carpenter, R. C.** (2019). Changes in coral reef community
818 structure in response to year-long incubations under contrasting pCO₂ regimes. *Mar.*
819 *Biol* **166**, 94.
- 820 **Fitt, W. K., Brown, B. E., Warner, M. E. and Dunne, R. P.** (2001). Coral bleaching:
821 interpretation of thermal tolerance limits and thermal thresholds in tropical corals. *Coral*
822 *Reefs* **20**, 51-65.
- 823 **Fitt, W. K., McFarland, F., Warner, M. E. and Chilcoat, G. C.** (2000). Seasonal patterns of
824 tissue biomass and densities of symbiotic dinoflagellates in reef corals and relation to
825 coral bleaching. *Limnol Oceanogr* **45**, 677-685.
- 826 **Glynn, P.** (1993). Coral reef bleaching: ecological perspectives. *Coral reefs* **12**, 1-17.
- 827 **Grottoli, A., Rodrigues, L. and Juarez, C.** (2004). Lipids and stable carbon isotopes in two
828 species of Hawaiian corals, *Porites compressa* and *Montipora verrucosa*, following a
829 bleaching event. *Mar. Biol* **145**, 621-631.
- 830 **Grottoli, A. G., Rodrigues, L. J. and Palardy, J. E.** (2006). Heterotrophic plasticity and
831 resilience in bleached corals. *Nature* **440**, 1186.
- 832 **Grottoli, A. G., Warner, M. E., Levas, S. J., Aschaffenburg, M. D., Schoepf, V., McGinley,**
833 **M., Baumann, J. and Matsui, Y.** (2014). The cumulative impact of annual coral
834 bleaching can turn some coral species winners into losers. *Global Change Biology* **20**,
835 3823-3833.
- 836 **Hoegh-Guldberg, O., Mumby, P. J., Hooten, A. J., Steneck, R. S., Greenfield, P., Gomez,**
837 **E., Harvell, C. D., Sale, P. F., Edwards, A. J. and Caldeira, K.** (2007). Coral reefs
838 under rapid climate change and ocean acidification. *science* **318**, 1737-1742.
- 839 **Holcomb, M., Cohen, A. L. and McCorkle, D. C.** (2012). An investigation of the calcification
840 response of the scleractinian coral *Astrangia poculata* to elevated pCO₂ and the effects of
841 nutrients, zooxanthellae and gender. *Biogeosciences* **9**, 29-39.
- 842 **Horvath, K. M., Castillo, K. D., Armstrong, P., Westfield, I. T., Courtney, T. and Ries, J. B.**
843 (2016). Next-century ocean acidification and warming both reduce calcification rate, but
844 only acidification alters skeletal morphology of reef-building coral *Siderastrea siderea*.
845 *Sci Rep.* **6**, 29613.
- 846 **Hughes, T. P., Kerry, J. T., Álvarez-Noriega, M., Álvarez-Romero, J. G., Anderson, K. D.,**
847 **Baird, A. H., Babcock, R. C., Beger, M., Bellwood, D. R. and Berkelmans, R.** (2017).
848 Global warming and recurrent mass bleaching of corals. *Nature* **543**, 373.
- 849 **Jokiel, P. and Coles, S.** (1990). Response of Hawaiian and other Indo-Pacific reef corals to
850 elevated temperature. *Coral reefs* **8**, 155-162.

- 851 **Jokiel, P., Rodgers, K., Kuffner, I., Andersson, A., Cox, E. and Mackenzie, F.** (2008). Ocean
852 acidification and calcifying reef organisms: a mesocosm investigation. *Coral reefs* **27**,
853 473-483.
- 854 **Jury, C. P., Whitehead, R. F. and Szmant, A. M.** (2010). Effects of variations in carbonate
855 chemistry on the calcification rates of *Madracis auretenra* (= *Madracis mirabilis* sensu
856 Wells, 1973): bicarbonate concentrations best predict calcification rates. *Global Change*
857 *Biology* **16**, 1632-1644.
- 858 **Kenkel, C., Goodbody-Gringley, G., Caillaud, D., Davies, S., Bartels, E. and Matz, M.**
859 (2013a). Evidence for a host role in thermotolerance divergence between populations of
860 the mustard hill coral (*Porites astreoides*) from different reef environments. *Mol Ecol* **22**,
861 4335-4348.
- 862 **Kenkel, C., Meyer, E. and Matz, M.** (2013b). Gene expression under chronic heat stress in
863 populations of the mustard hill coral (*Porites astreoides*) from different thermal
864 environments. *Mol Ecol* **22**, 4322-4334.
- 865 **Kenkel, C. D. and Matz, M. V.** (2016). Gene expression plasticity as a mechanism of coral
866 adaptation to a variable environment. *Nat. Ecol. Evol.* **1**, 0014.
- 867 **Kleypas, J. A., Buddemeier, R. W., Archer, D., Gattuso, J.-P., Langdon, C. and Opdyke, B.**
868 **N.** (1999). Geochemical consequences of increased atmospheric carbon dioxide on coral
869 reefs. *science* **284**, 118-120.
- 870 **Kline, D. I., Teneva, L., Okamoto, D. K., Schneider, K., Caldeira, K., Miard, T., Chai, A.,**
871 **Marker, M., Dunbar, R. B. and Mitchell, B. G.** (2019). Living coral tissue slows
872 skeletal dissolution related to ocean acidification. *Nat. Ecol. Evol.* **3**, 1438-1444.
- 873 **Kornder, N. A., Riegl, B. M. and Figueiredo, J.** (2018). Thresholds and drivers of coral
874 calcification responses to climate change. *Global change biology* **24**, 5084-5095.
- 875 **Kroeker, K. J., Kordas, R. L., Crim, R., Hendriks, I. E., Ramajo, L., Singh, G. S., Duarte,**
876 **C. M. and Gattuso, J. P.** (2013). Impacts of ocean acidification on marine organisms:
877 quantifying sensitivities and interaction with warming. *Global change biology* **19**, 1884-
878 1896.
- 879 **Kroeker, K. J., Kordas, R. L., Crim, R. N. and Singh, G. G.** (2010). Meta-analysis reveals
880 negative yet variable effects of ocean acidification on marine organisms. *Ecol Lett* **13**,
881 1419-1434.
- 882 **LaJeunesse, T. C., Parkinson, J. E., Gabrielson, P. W., Jeong, H. J., Reimer, J. D., Voolstra,**
883 **C. R. and Santos, S. R.** (2018). Systematic revision of Symbiodiniaceae highlights the
884 antiquity and diversity of coral endosymbionts. *Curr Biol* **28**, 2570-2580. e6.
- 885 **Lê, S., Josse, J. and Husson, F.** (2008). FactoMineR: an R package for multivariate analysis.
886 *Journal of statistical software* **25**, 1-18.
- 887 **Levas, S., Schoepf, V., Warner, M. E., Aschaffenburg, M., Baumann, J. and Grottoli, A. G.**
888 (2018). Long-term recovery of Caribbean corals from bleaching. *J. Exp. Mar. Biol. Ecol*
889 **506**, 124-134.
- 890 **Marchetti, A., Schruth, D. M., Durkin, C. A., Parker, M. S., Kodner, R. B., Berthiaume, C.**
891 **T., Morales, R., Allen, A. E. and Armbrust, E. V.** (2012). Comparative
892 metatranscriptomics identifies molecular bases for the physiological responses of
893 phytoplankton to varying iron availability. *Proceedings of the National Academy of*
894 *Sciences* **109**, E317-E325.

- 895 **Masuko, T., Minami, A., Iwasaki, N., Majima, T., Nishimura, S.-I. and Lee, Y. C.** (2005).
896 Carbohydrate analysis by a phenol–sulfuric acid method in microplate format. *Analytical*
897 *biochemistry* **339**, 69-72.
- 898 **Matz, M. V., Treml, E. A., Aglyamova, G. V. and Bay, L. K.** (2018). Potential and limits for
899 rapid genetic adaptation to warming in a Great Barrier Reef coral. *PLoS genetics* **14**,
900 e1007220.
- 901 **Mayorga-Adame, C. G., Batchelder, H. P. and Spitz, Y.** (2017). Modeling larval connectivity
902 of coral reef organisms in the Kenya-Tanzania region. *Frontiers in Marine Science* **4**, 92.
- 903 **McLachlan, R. H., Price, J. T., Solomon, S. L. and Grotto, A. G.** (2020). Thirty years of
904 coral heat-stress experiments: a review of methods. *Coral Reefs*, 1-18.
- 905 **Morley, J. W., Selden, R. L., Latour, R. J., Frölicher, T. L., Seagraves, R. J. and Pinsky, M.**
906 **L.** (2018). Projecting shifts in thermal habitat for 686 species on the North American
907 continental shelf. *PLoS one* **13**, e0196127.
- 908 **Muscattine, L.** (1990). The role of symbiotic algae in carbon and energy flux in reef corals.
909 *Ecosystems of the world. Coral Reefs*.
- 910 **Nakagawa, S. and Schielzeth, H.** (2013). A general and simple method for obtaining R² from
911 generalized linear mixed-effects models. *Methods in ecology and evolution* **4**, 133-142.
- 912 **Nunes, F. L., Norris, R. D. and Knowlton, N.** (2011). Long distance dispersal and connectivity
913 in amphiatlantic corals at regional and basin scales. *PLoS one* **6**, e22298.
- 914 **Okazaki, R. R., Towle, E. K., van Hooidonk, R., Mor, C., Winter, R. N., Piggot, A. M.,**
915 **Cunning, R., Baker, A. C., Klaus, J. S. and Swart, P. K.** (2017). Species-specific
916 responses to climate change and community composition determine future calcification
917 rates of Florida Keys reefs. *Global change biology* **23**, 1023-1035.
- 918 **Oksanen, J.** (2011). Vegan: community ecology package. R package ver. 2.0-2. [http://CRAN.R-](http://CRAN.R-project.org/package=vegan)
919 [project.org/package=vegan](http://CRAN.R-project.org/package=vegan).
- 920 **Oliver, T. and Palumbi, S.** (2011). Do fluctuating temperature environments elevate coral
921 thermal tolerance? *Coral Reefs* **30**, 429-440.
- 922 **Orr, J. C., Fabry, V. J., Aumont, O., Bopp, L., Doney, S. C., Feely, R. A., Gnanadesikan,**
923 **A., Gruber, N., Ishida, A. and Joos, F.** (2005). Anthropogenic ocean acidification over
924 the twenty-first century and its impact on calcifying organisms. *Nature* **437**, 681.
- 925 **Palumbi, S. R., Barshis, D. J., Traylor-Knowles, N. and Bay, R. A.** (2014). Mechanisms of
926 reef coral resistance to future climate change. *Science* **344**, 895-898.
- 927 **Parmesan, C. and Yohe, G.** (2003). A globally coherent fingerprint of climate change impacts
928 across natural systems. *Nature* **421**, 37.
- 929 **Pörtner, H., Roberts, D., Masson-Delmotte, V., Zhai, P., Tignor, M., Poloczanska, E.,**
930 **Mintenbeck, K., Nicolai, M., Okem, A. and Petzold, J.** (2019). IPCC Special Report on
931 the Ocean and Cryosphere in a Changing Climate. *IPCC Intergovernmental Panel on*
932 *Climate Change: Geneva, Switzerland*.
- 933 **Prada, F., Caroselli, E., Mengoli, S., Brizi, L., Fantazzini, P., Capaccioni, B., Pasquini, L.,**
934 **Fabricius, K., Dubinsky, Z. and Falini, G.** (2017). Ocean warming and acidification
935 synergistically increase coral mortality. *Sci Rep.* **7**, 1-10.
- 936 **R Core Team.** (2017). R: A language and environment for statistical computing. Vienna,
937 Austria.
- 938 **Reynaud, S., Leclercq, N., Romaine-Lioud, S., Ferrier-Pagés, C., Jaubert, J. and Gattuso,**
939 **J. P.** (2003). Interacting effects of CO₂ partial pressure and temperature on

- 940 photosynthesis and calcification in a scleractinian coral. *Global Change Biology* **9**, 1660-
941 1668.
- 942 **Ries, J., Cohen, A. and McCorkle, D.** (2010). A nonlinear calcification response to CO₂-
943 induced ocean acidification by the coral *Oculina arbuscula*. *Coral Reefs* **29**, 661-674.
- 944 **Ries, J. B.** (2011). A physicochemical framework for interpreting the biological calcification
945 response to CO₂-induced ocean acidification. *Geochim. Cosmochim. Acta* **75**, 4053-4064.
- 946 **Rodolfo-Metalpa, R., Houlbrèque, F., Tambutté, É., Boisson, F., Baggini, C., Patti, F. P.,
947 Jeffree, R., Fine, M., Foggo, A. and Gattuso, J.** (2011). Coral and mollusc resistance to
948 ocean acidification adversely affected by warming. *Nat. Clim. Change*. **1**, 308.
- 949 **Rodolfo-Metalpa, R., Peirano, A., Houlbrèque, F., Abbate, M. and Ferrier-Pagès, C.** (2008).
950 Effects of temperature, light and heterotrophy on the growth rate and budding of the
951 temperate coral *Cladocora caespitosa*. *Coral Reefs* **27**, 17-25.
- 952 **Rodrigues, L. J. and Grottoli, A. G.** (2007). Energy reserves and metabolism as indicators of
953 coral recovery from bleaching. *Limnol Oceanogr* **52**, 1874-1882.
- 954 **Roth, M. S.** (2014). The engine of the reef: photobiology of the coral-algal symbiosis. *Front*
955 *Microbiol.* **5**, 422.
- 956 **Rueden, C. T., Schindelin, J., Hiner, M. C., DeZonia, B. E., Walter, A. E., Arena, E. T. and
957 Eliceiri, K. W.** (2017). ImageJ2: ImageJ for the next generation of scientific image data.
958 *BMC bioinformatics* **18**, 529.
- 959 **Schoepf, V., Grottoli, A. G., Levas, S. J., Aschaffenburg, M. D., Baumann, J. H., Matsui, Y.
960 and Warner, M. E.** (2015). Annual coral bleaching and the long-term recovery capacity
961 of coral. *Proceedings of the Royal Society B: Biological Sciences* **282**, 20151887.
- 962 **Schoepf, V., Grottoli, A. G., Warner, M. E., Cai, W.-J., Melman, T. F., Hoadley, K. D.,
963 Pettay, D. T., Hu, X., Li, Q. and Xu, H.** (2013). Coral energy reserves and calcification
964 in a high-CO₂ world at two temperatures. *PloS one* **8**, e75049.
- 965 **Schoepf, V., Jury, C. P., Toonen, R. J. and McCulloch, M. T.** (2017). Coral calcification
966 mechanisms facilitate adaptive responses to ocean acidification. *Proceedings of the Royal*
967 *Society B: Biological Sciences* **284**, 20172117.
- 968 **Shaw, E. C., Carpenter, R. C., Lantz, C. A. and Edmunds, P. J.** (2016). Intraspecific
969 variability in the response to ocean warming and acidification in the scleractinian coral
970 *Acropora pulchra*. *Mar. Biol* **163**, 210.
- 971 **Stevens, G. C.** (1989). The latitudinal gradient in geographical range: how so many species
972 coexist in the tropics. *Am. Nat.* **133**, 240-256.
- 973 **Thomas, L., Rose, N. H., Bay, R. A., López, E. H., Morikawa, M. K., Ruiz-Jones, L. and
974 Palumbi, S. R.** (2018). Mechanisms of thermal tolerance in reef-building corals across a
975 fine-grained environmental mosaic: Lessons from Ofu, American Samoa. *Frontiers in*
976 *Marine Science* **4**, 434.
- 977 **Towle, E. K., Enochs, I. C. and Langdon, C.** (2015). Threatened Caribbean coral is able to
978 mitigate the adverse effects of ocean acidification on calcification by increasing feeding
979 rate. *PloS one* **10**, e0123394.
- 980 **Warner, M. E., Fitt, W. K. and Schmidt, G. W.** (1999). Damage to photosystem II in
981 symbiotic dinoflagellates: a determinant of coral bleaching. *Proceedings of the National*
982 *Academy of Sciences* **96**, 8007-8012.
- 983 **Weis, V. M.** (2008). Cellular mechanisms of Cnidarian bleaching: stress causes the collapse of
984 symbiosis. *J. Exp. Biol.* **211**, 3059-3066.
- 985